NTNU
Det skapende universitet

Utmatting av komposittrør med boltforbindelser

Marcus Vincent Horn

MASTER THESIS SPRING 2016
FOR
STUD.TECHN. MARCUS HORN

Fatigue of Composite Pipes with Bolted Joints

Utmattelse av kompositt rør med bolt forbindelser

Pipes and tubes are major components used in the offshore and processing industry.
This project shall investigate novel ways to make and join composite pipes. Pipes will be
produced with the filament winding machines. Metal end fittings will be attached with bolts.
Fatigue properties will be tested and analyzed.

Formal requirements:

Three weeks after start of the thesis work, an A3 sheet illustrating the work is to be handed
in. A template for this presentation is available on the IPM's web site under the menu
"Masteroppgave" (https://www.ntnu.edu/web/ipm/master-thesis). This sheet should be
updated one week before the master's thesis is submitted.

Risk assessment of experimental activities shall always be performed. Experimental work
defined in the problem description shall be planed and risk assessed up-front and within 3
weeks after receiving the problem text. Any specific experimental activities which are not
properly covered by the general risk assessment shall be particularly assessed before
performing the experimental work. Risk assessments should be signed by the supervisor
and copies shall be included in the appendix of the thesis.

The thesis should include the signed problem text, and be written as a research report with
summary both in English and Norwegian, conclusion, literature references, table of
contents, etc. During preparation of the text, the candidate should make efforts to create a
well arranged and well written report. To ease the evaluation of the thesis, it is important to
cross-reference text, tables and figures. For evaluation of the work a thorough discussion of
results is appreciated.

The thesis shall be submitted electronically via DAIM, NTNU's system for Digital Archiving
and Submission of Master's theses.

Torgeir Welo
Head of Division

Andreas Echtermeyer
Professor/Supervisor

NTNU
Norges teknisk-
naturvitenskapelige universitet
Institutt for produktutvikling
og materialer

Preface

This master thesis in mechanical engineering has been written at NTNU as part of the study program Engineering materials and design. It has been a continuation of my project thesis and was carried out in the spring semester of 2016. The work regarding the thesis has been an immense learning experience for me as I have been responsible for every operation that has been done in the study, including production of samples, testing and analyzing.

I would like to thank Andreas Echtermeyer. His guidance and knowledge was of great value throughout the entire project. Carl-Magnus Midtbø and Børge Holen also deserves much gratitude for their assistance every time I made metal fail instead of composites. I would like to thank Erik Sæter for all the hours we spent solving different problems in the lab. Additionally, it made me very confident to know that I could always ask for help or discuss issues with Nils Petter Vedvik, Kaspar Lasn, Søren Heinze, Sondre Landvik and Daniel Tran.

This year would not have been the same without Jenny and my fellow students at Kunnskapsklyngen (KuK). Thank you for making it so memorable.

Trondheim, 2016-06-09

Marcus Horn

Abstract

A system for connecting composite tubes to metal structures has been developed at NTNU. The solution consists of a metal end fitting with radially inserted bolt connections. The response of a composite structure to cyclic tensile loading when connected to the metal end fittings has been investigated. The objective for the research is to obtain the ability to predict the lifetime of such structures. Strain measurements by an optical backscatter reflectometer interrogator and optical fibers have been evaluated for use as structural health monitoring. A filament wounded glass fiber reinforced epoxy tube with quasi-isotropic layup has been modified to accommodate for the bolt connections. Data was acquired through strain gauges, linear variable differential transformers, distributed fiber optic sensing and a load cell. The final results are based on two static tensile tests and six dynamic tensile tests. The dynamic tests were conducted at a frequency of 4 Hz with a R-ratio of 0.1. The maximum loads were 70 kN, 80 kN, 90 kN and 100 kN, which corresponds to 46.7%, 53.3%, 60% and 66.7% of the critical load. The research has resulted in a S-N curve which has been successfully curve fitted to DNV specifications. A method to monitor the structural health through the use of optical fibers and optical backscatter reflectometry has been evaluated. It proved to be a useful method for monitoring the load distribution on the respective bolt holes. Several fatigue models for lifetime prediction is explored. The models are based on residual stiffness, crushing rate and critical load and displacements.

Sammendrag

Ett system for å koble komposittrør opp mot metallstrukturer har blitt utviklet ved NTNU. Løsningen består av ett metallendestykke med bolter skrudd inn radielt. Egenskapene til et komposittrør koblet opp til to metallendestykker og utsatt for sykliske strekklaster har blitt undersøkt. Formålet med studiet er å kunne forutse levetiden til slike strukturer. Tøyningsmålinger ved hjelp en fiber optiske målinger har blitt undersøkt for bruk i strukturell helseovervåking. Ett viklet glassfiberforsterket epoksyrør med kvasi-isotropisk stablekombinasjon av fiber har blitt modifisert for å kunne kobles opp mot metallendestykkene. Data ble innhentet fra strekklapper, differentialtransformatorer, fiber optikk og en lastcelle. Resultatene er basert på to statiske strekktester og seks dynamiske strekktester. De dynamiske testene ble utført med en frekvens på 4 Hz og en R-ratio på 0.1. Makslastene som de dynamiske testene ble utført ved var 70 kN, 80 kN, 90 kN og 100 kN. Dette tilsvarer 46.7%, 53.3%, 60% og 66.7% av den kritiske lasten. Studiet resulterte i tre alternative S-N kurver. I tillegg ble flere modeller for utmattingslivet utforsket. Modellene er basert på reststivhet, knuserate og kritiske laster og forskyvninger. For å kunne evaluere styrken til strukturen under drift har en metode som utnytter optiske fibre har blitt vurdert. Resultatene viser at det er mulig å utnytte metoden for å kunne forstå lastfordelingen over de respektive bolthullene i komposittrøret.

Contents

Chapter 1

Introduction

In order to optimize structures with respect to function, weight, ease of production etc. it is often desired to combine parts of metals and composites. Metal composite connections is one of the larger focus areas with regards to composites in the industry today. A solution to connect composite pipes to pipe extensions or to metal structures has been developed at NTNU. It has been done through the work of Karsten Dons (Dons, 2013) and Anders Fosså (Fosså, 2014), under the supervision of Andreas Echtermeyer. See Figure 1.1 The joining principle is based on bolt connections, which can be seen from the assembly overview in 1.2a and the description in Table 1.2b The design has been governed by optimization for fluid transportation. Sealing is ensured through the O-ring solution shown in Figure 1.3. The final design, see Figure 1.1, is also meant to ensure proper flow of the transported fluids. All figures in this chapter have been retrieved from Fosså (2014).
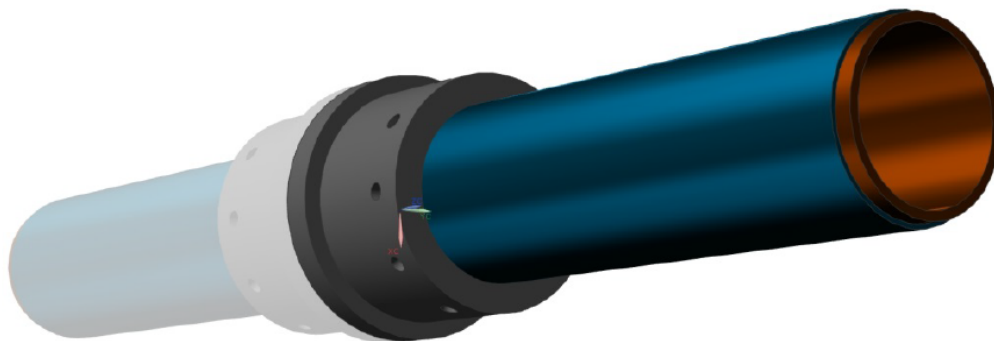
Figure 1.1: Concept model of the proposed design. Source: Fosså (2014)

(b) Description of components in Fig. 1.2a
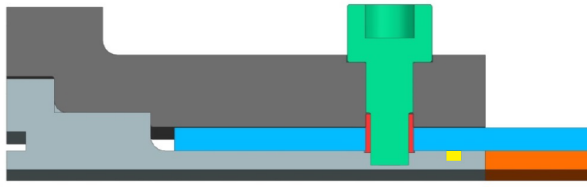
(a) Assembly drawing of one proposed concept. In the final design the outer flange and the flange core is one single part. Source: Fosså (2014)

Color	Component
Dark grey	Outer flange
Light grey	Flange core
Red	SKF bushing
Green	M12 bolt
Blue	GFRP tube
Orange	PE liner
Yellow	O-ring

Figure 1.2
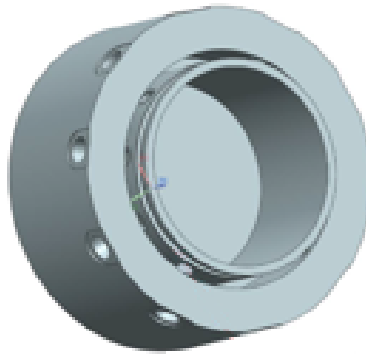
Figure 1.3: CAD-model of the metal end fitting. Source: Fosså (2014)

This thesis falls within the second stage of the building block approach, see Figure 1.4. The tests performed in this study will be performed in order to evaluate parts of a larger system. This thesis will serve to support the overall design project with fatigue data and alternatives for structural health monitoring.
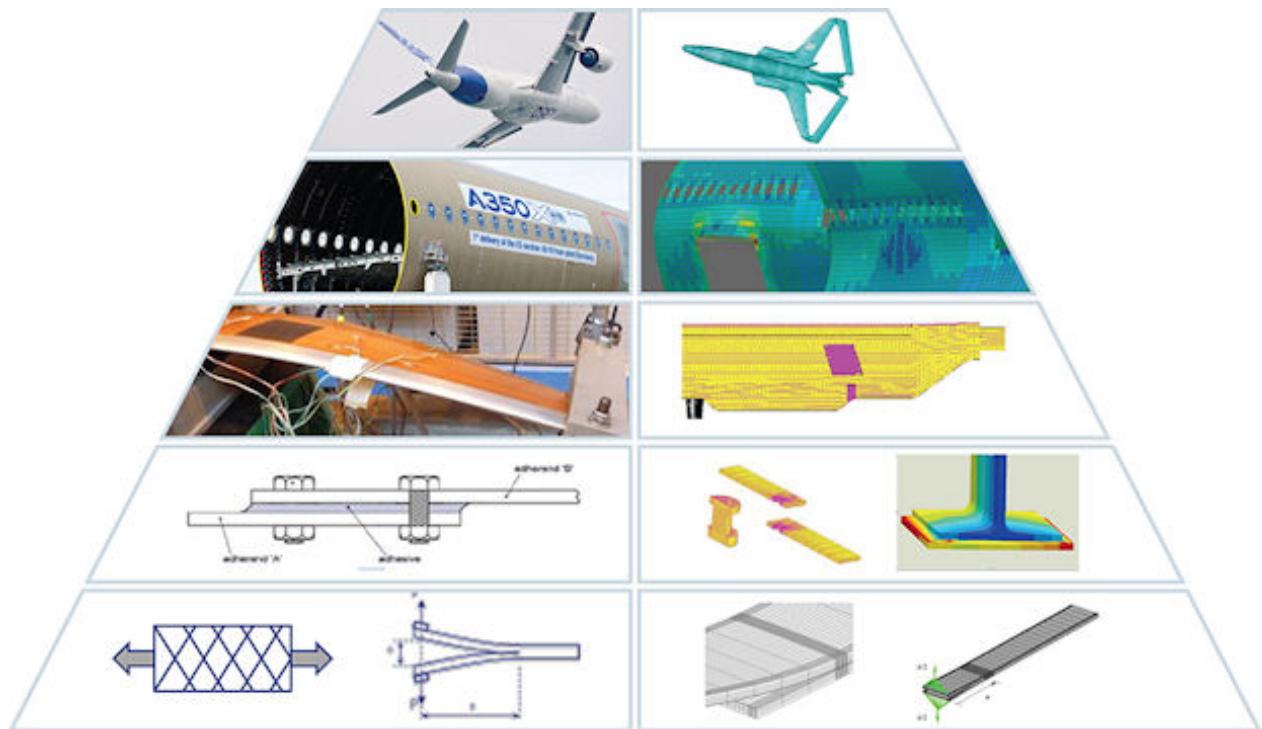
Figure 1.4: The building block approach. In order to reduce cost this approach is followed. In the first step, the smallest components of a system are tested thoroughly. Then throughout the next steps, the number of tests are gradually reduced as the systems becomes more complex. Source: Lecture notes produced for the course MTRL594: Advanced Composite Materials, at UBC Vancouver

Chapter 2

Theory

2.1 Composite metal interface / transition

The increased use of composites in the transport sector (e.g. airplanes and cars) and the energy sector (e.g. windmills) has turned a large focus towards finding solutions for joining composite structures with metal structures. Joining of dissimilar materials may be done in several different ways, depending on the application and materials. The different convenient methods are based on the principles of adhesion, welding and mechanical fastening (Kah et al., 2014). Mechanical fastening is the only group which enables the opportunity to also disassemble the joint. The joining methods normally incorporates clamps or bolts. These methods are considered simple, convenient and they do not require much resources such as welding machines or large ovens. According to Bhandari (Bhandari, 2001), these are some of the reasons for why mechanical fastening is the most commonly used technique for joining components. Nevertheless, there are some important side effects. Bolt connections, which is the focus of this study, do increase the number of components in an assembly as well as inducing stress concentrations around the bolt holes.

2.2 Bolt holes in a laminate

2.2.1 Typical failures

When designing a bolt hole there are several factors which must be considered. These factors are best explained through the different failure modes. Figure 2.1 displays the different scenarios in which a structure may fail when subjected to loading perpendicular to the bolt.
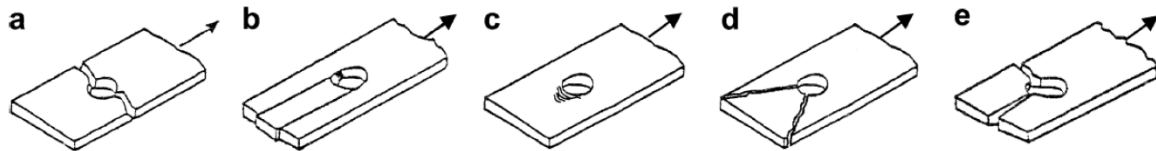
Figure 2.1: Failure modes for composites with bolt holes: a) net tension, b) shear out, c) bearing failure, d) tear out and e) cleavage. Source: Fosså (2014).

In scenario "a) net tension failure", the notch effect plays a large role. First of all, cross sectional area is removed when drilling a bolt hole in the structure. Which means that the larger the diameter of the hole, the smaller the cross section around the hole becomes. This leads to an increase in stress in the respective area. Additionally, the area around the hole will exhibit stress concentrations due to the notch effect, which is represented by the graph in Figure 2.2. The high local stress concentration, possibly combined with surface defects will create a natural point for crack initiation perpendicular to the loading direction.
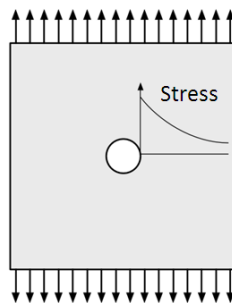
Figure 2.2: Stress concentration due to the notch effect. Source: Leancrew.com, "Cracked" 04.02.16 14:00

If the diameter of the hole becomes relatively small, then the cross section around a hole will be large enough to retain the loading. On the other hand, if the load transferred from the bolt to the composite is large enough and the diameter is small enough it will cause shear out (Fig.

2.1b). With crack initiation points near the hole midpoint, for the same reason as previously. Then shear forces cause the crack to propagate in the loading direction. This failure mechanism is difficult to predict accurately due to the multiaxial stress state near the bolt hole (Thoppul et al., 2009).

The last of the three primary failure modes is bearing failure (Fig. 2.1c). It is a non-catastrophic failure mode, which occurs gradually. Bearing failure is governed by the compressive forces caused by the bolt. It is the primary failure mode caused by fatigue of bolted connections. This mechanism may lead to other secondary failures such as tear-out or cleavage (Fig. 2.1 d and e). Prediction of these failures are dependent on different ratios with regards to the geometry.

2.2.2 Geometrical ratios

The e/d-ratio and the w/d-ratio describes geometrical relationships. The e/d-ratio describes the ratio between the hole diameter (d) and the distance towards the edge in the load direction (e). The w/d-ratio describes the ratio between the hole diameter and the distance between two holes aligned perpendicular to the load direction (w). The relationship between the two ratios can be used to determine the failure mode. For isotropic structures a high e/d and low w/d will result in tear out, whilst an opposite situation will result in shear out.

Based on previous testing, bearing failure and shear out are the two most important failure mechanisms to consider for the given system and applied loading. Also when considering the failure, it is important to look at it from a composite point of view. This will be further emphasized on with regards to fatigue.

2.3 Fatigue

Fatigue failure occurs when a structure is subjected to cyclic loading. The loading may either be alternating between tension and compression, or pulsating in either compression or tension. Loading cycles are classified based on its mean load, the load amplitude and the R-ratio seen below, see Figure 2.3 and Equation 2.1.

The fatigue properties of composite tubes are rather complex. In previous studies, load conditions are normally considered as uniaxial or biaxial, whereas the different loadings may be
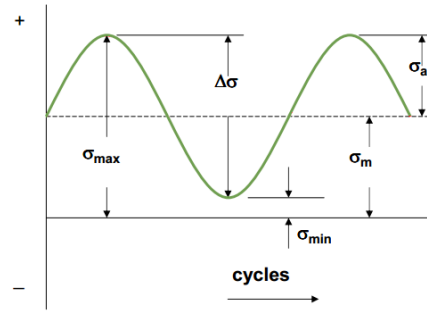
Figure 2.3: Graphic representation of cyclic loading. The scenario shown is pulsating tensile loading

axial tension/compression, torsion, bending or internal/external pressure. For every different loading vector there is a different preferred lay-up. The fatigue properties of composite tubes have previously been studied, but are normally limited to a common lay-up and loading scenario. There is a vast amount of ways to study composite tubes. Among some, Perreux et al. (Perreux and Joseph, 1997) and Kaynak and Mat (Kaynak and Mat, 2001) studied $[+55/-55]_n$ tubes in uniaxial tensile loading in order to identify the characteristics the fatigue behavior.

In this thesis it is desired to look at the fatigue properties of composite tubes. The tubes are connected to a metal end fitting through bolted connections. They will be subjected to tensile cyclic fatigue, meaning that the maximum load and the R-ratio is higher than zero (Equation 2.1). The load cycle will be based on results from tensile tests and a chosen R-ratio. Fosså (Fosså, 2014) used a maximum dynamic load equal to 80% of the maximum static load.

$$R = \frac{\sigma_{min}}{\sigma_{max}} \tag{2.1}$$

The loading frequency is normally chosen based on its effect on the materials and test practicalities. Perreux et al. (Perreux and Joseph, 1997) studied the effects of frequency on fatigue loading of composites. The results proved that frequency may have a significant influence on the test results. A low frequency (around 0.1 Hz) will result in a higher time-under-load which will result in effects of a time dependent failure mechanism, such as creep. This will then result in fewer cycles before failure. On the other hand, a high frequency (approximately 10 Hz) will result in heat generation, which increase the degradation of the material. It is therefore meaningful to choose the highest possible frequency which will not cause radical heat generation.

Previous similar testing conducted at NTNU has been run at 2-4 Hz.

2.3.1 Failure mechanisms and prediction

Predictions of failure due to fatigue may be rather complex. For various types of metals there are well-established models based on thorough testing and analyzing. Fatigue in composites is rather complicated to predict with a global model, because of the wide range of configurations and material combinations.

There have been several studies which have focused on the failure development on both micro scale and macro scale. It has been shown that most of the failures occur at an early stage in the matrix (Perreux and Joseph, 1997). Because of the brittleness of the matrix and relatively low strength it will crack at a low strain. Matrix cracking is therefore the first damage mechanism. These cracks / crazes will have a small but considerable effect on the overall strength.

Kaynak and Mat (Kaynak and Mat, 2001) studied failure developments for relatively similar systems and loads. For example, with a frequency of 1 Hz and a maximum loading at 80% of the ultimate loading they showed that weakening due to matrix cracks would occur after approximately 40 cycles. After/during matrix cracking, debonding at the interface between the matrix and the fibers was observed after 100 cycles. Fiber failure did occur after 200 cycles and ultimate failure occurred after 2000 cycles.

In addition to frequency and loading there are several other factors to consider when estimating lifetime. According to Saunders et al. (Saunders et al., 1993) the removal of bolts during the lifetime of the structure may accelerate crack propagation because fatigue debris will fall out. Persson et al. (Persson et al., 1997) studied the effects of hole machining defects on fatigue life. They also proposed a method for producing defect free holes. Fosså (Fosså, 2014) showed that if the tube was constrained in the thickness direction, it could cause an increase in stiffness as well as stress concentrations around the hole, due to out-of-plane effects.

Due to the vast amounts of variables which can affect the fatigue life it has been decided to conduct a relatively thorough study on different ways to predict fatigue failure of the given composite structure.

2.3.2 Fatigue life analysis

In chapter 7. of Damage and Failure of Composite Materials (Talreja and Singh, 2012) it is evaluated whether empiricism based or mechanisms based fatigue modelling is more suitable for composites. Much of the preliminary studies with either fatigue of metals or composites are often based on empiricism. Due to the vast amount of combinations in material properties it is stated that mechanisms based modeling is the only rational approach to fatigue in composites. On the other hand, one of the most common ways to predict the lifetime of metals subjected to fatigue is through the use of Paris' law. Paris' law is used to curve fit to observed crack data due to cyclic crack growth. See Figure 2.4 for example.
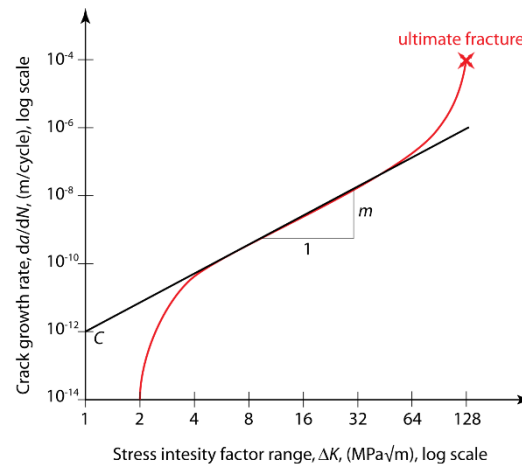
Figure 2.4: The linear area on the graph shows the area which is represented by Paris' Law. Source: Wikipedia.org, "Paris Law" 25.01.16 13:00

Another common way to describe the fatigue lifetime is through S-N curves. These curves are also based on empirical data and shows the relation between mean loading cyclic loading and lifetime. Cox et al. (2014) and Samborsky et al. (2009) evaluated failure as a rapid increase in compliance increase versus the number of cycles. Thereafter the number of cycles to failure and respective stresses were plotted to create a S-N curve. Lines were fitted with a power law based on Equation 2.2 where N is the number of cycles to failure, K and m are material coefficients.

$$N = K * \sigma^{-m} \tag{2.2}$$

Several studies, such as the work by Joseph and Perreux (1994) have used the Wohler curve

complimented with a stiffness loss model. They showed that the curve could be described by the function

$$\sigma_{\text{mean}} = A + B * log(N_f) \tag{2.3}$$

where B is considered a constant, while

$$A = \alpha + \beta * log(frequency) \tag{2.4}$$

Additionally, they found a relationship between the stiffness loss and n cycles. Based on their results, they assume that the damage variable D, is estimated through the Equation 2.5

$$D = \frac{E_0 - E}{E_0} \tag{2.5}$$

and that the experimental results show that $D = D(\sigma_M, frequency, n)$. Finally, their work results in a cumulative damage law which states that, independent of stress level but dependent of frequency, the following equation (Eq. 2.6) can be utilized.

$$\frac{E}{E_0}(frequency) = F(\frac{n}{N_f}) \tag{2.6}$$

As described by Talreja and Singh (2012), another method proposed by Hahn and Kim is based on the strain versus cycle relationship. A similar idea seems to have been further investigated by Lee and Hwang (2000). In "Fatigue Life Prediction of Matrix Dominated Polymer Composite Material" they describe fatigue life prediction based on the so-called fatigue modulus.

For fiber dominated laminates the failure of fatigue is mainly dependent on the maximum strain. This is shown in Figure 2.5. The fatigue modulus is given as

$$F(n, q) = \frac{q}{\epsilon_n} \tag{2.7}$$

where ϵ_n is the strain at a given cycle and q is the ratio of applied stress to the ultimate stress. Through empirical testing it may be possible to identify the degradation rate of the fatigue mod-

ulus. The degradation rate per cycle is defined as the power function

$$\frac{dF(n,q)}{dn} = -F_0 * a * C * n^{c-1} \tag{2.8}$$

Where a and C are material constants, F_0 is the fatigue modulus at the first cycle and n is number of cycles. By knowing the maximum strain and the applied load, it is thereby possible to estimate the lifetime.
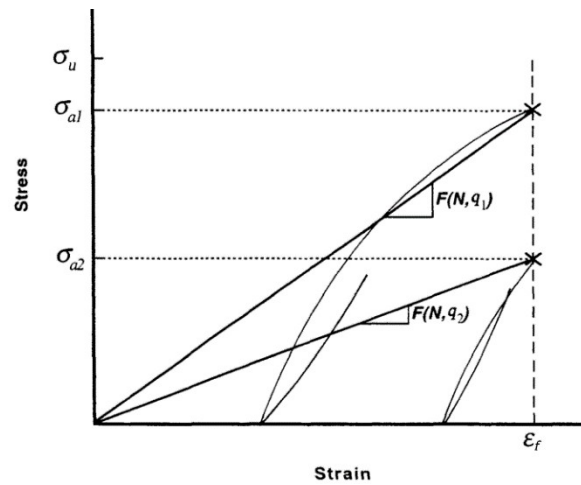
Figure 2.5: Fatigue modulus at failure cycle. $F(N,q)$ denotes the fatigue modulus, ϵ_f and σ_u denotes the ultimate strain and stress, σ_a denotes the applied stress. Source: Lee and Hwang (2000)

In the preliminary studies (Horn, 2015) certain trends throughout the fatigue life cycles were found. By evaluating the system stiffness at different intervals throughout the life, it was discovered that the stiffness does increase with the first (1-5 or 10) cycles, then it remains relatively static throughout the remaining lifetime. Additionally, it was observed that the sample undergoes three different phases, see Fig. 2.6. In phase 1, the initiation phase, the crushing rate (CR) is high and although which results in a large displacement despite the relatively low number of cycles. In phase 2, the system is stable. Most of the life is in this phase, and can be assumed to have a linear crushing rate. The final phase is when the crushing rate is increasing radically. This phase start at a critical displacement or number of cycles.
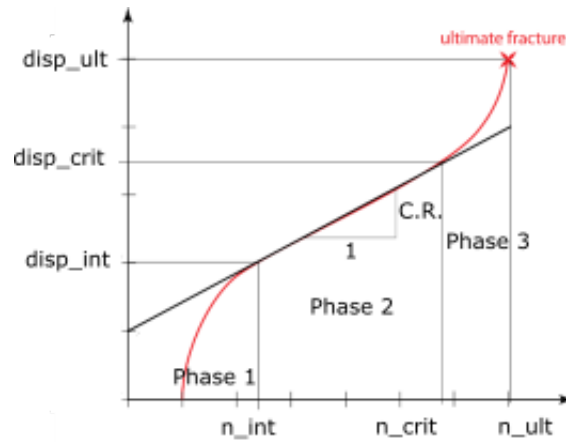
Figure 2.6: Overview of variables and sections

2.4 Structural health monitoring

The demand for composite materials in the industry is increasing due to its many beneficial properties such as the high strength to weight ratio. A downside to composites is that there are still unknowns regarding the behavior and failure modes of composites. Hence, it needs to be predicted or monitored properly. According to Manyika et al. (2015) the emerge of internet of things (IoT) will eventually change the maintenance model from repair and replace to predict and prevent. This change is possible through sensors which are placed onto or embedded into systems and objects in order to monitor their behavior while it is in use. Among the many alternatives to monitor the strain in a structure a distributed fiber optic sensing method has been chosen.

By embedding optical fibers or placing them on the surface of the laminate it is possible to accurately measure strain by using an optical backscatter reflectometer interrogator (Grave et al., 2015). Grave et al. (2015) used the respective technologies to measure the change in strain fields related to failure of adhesive joints. He found that changes in the strain field can be related to damage development and can be used for structural health monitoring (SHM). Strathman et al. (2016) surface mounted optical fibers to a composite wing in order to quantify the wing characteristics. They concluded that optical fibers could be useful in quantifying wing characteristics and also for evaluating structural health and crack growth throughout the life time. Fosså (2014) proposed a method for SHM with OBR by winding the optical fibers in hoop

around the tube in order to utilize it for damage prediction or detection. This method will be further investigated in this study.

2.5 Theory vs. empiricism

Composites are complex systems which are difficult to predict. Many studies have been conducted regarding modelling of fatigue in composites, but there have been found no well-established universal methods in textbooks for materials science. The essence of fatigue modeling is to be able to predict the full lifetime or remaining lifetime of a structure. The structure may be exposed to different loading scenarios, based on combinations of force and surrounding environment. There are several different ways to model the fatigue. Whether the model may be based on a theoretical or an empirical approach. In this study I will rely on empirical research in order to establish an understanding of the fatigue properties of the tube.

Chapter 3

Model and Simulation

The main scope of the project is to be able to predict the lifetime of the system which is studied based on different cyclic loadings. The model(s) will be based on empirical data and failure at macro scale. Although the system is subjected to cyclic tensile loading, the critical area is also subjected to cyclic compressive loading because of the bolt joints. Hence, on macro scale it is important to consider crack propagation from and deformation of the hole due to tensile loading and crushing of the laminate due to compressive loading. A main goal of the project is to establish an S-N curve in order to achieve an estimate of the lifetime of the composite based on different loadings. Additionally, I intend to explore different fatigue models to evaluate whether it is possible to use or modify a model to predict the remaining lifetime based on structural health monitoring.

3.1 S-N and S-D curves

As mentioned, S-N curves is a common tool for fatigue analysis. In this study, I intend to utilize S-N curves both for the initiation process of the crack/damage and complete failure. Useful data to acquire is the amount of cycles before failure (n_{ult}) and the displacement at failure for different loads (D_{ult}). Additionally, the displacement and cycles after phase 1 and 2 will also be logged. See Figure 2.6.

Based on different studies there are several ways to curve fit the fatigue data. In this study, a power law fit (Eq. 3.1, Cox et al. (2014) and Samborsky et al. (2009)), a semi-logarithmic fit (Eq.

3.2, Joseph and Perreux (1994)) and the recommended fit based on DNV-GL (2013) (Eq. 3.3) will be explored.

$$S = a * N^b \tag{3.1}$$

$$S = a - b * logN \tag{3.2}$$

$$logS = log\sigma_{0fatigue} - \alpha * logN \tag{3.3}$$

3.2 Lifetime analysis

As cyclic loading occur the composite will become delaminated and suffer from matrix cracking, splitting and fiber failure. In the preliminary studies (Horn, 2015) I explored methods such as evaluating the stiffness, maximum displacement and maximum strain after certain cycle intervals. The different results may be used in combination with established fatigue models.

3.2.1 Residual stiffness based model

The proposed residual stiffness based model relates to the same principle as the fatigue modulus described in the Chapter 2 Theory. Although the fatigue modulus is not similar because it is not originally meant for such a system which is tested in this study, the idea is transferable. It was found that, except from the first cycles, the variation in stiffness throughout most of the lifetime is negligible (Horn, 2015). By combining a set of parameters it should be possible to estimate the remaining cycles in the life of a system (c_{crit}). The parameters which are considered are the system stiffness (E_{system}), the maximum applied force (F_{max}), a critical displacement (D_{ph2}) and an initiation or current displacement (D_{ph1}). The model for calculating remaining cycles is shown in Eq. 3.4.

$$c_{crit} = D_{ph2} - D_{ph1} - (\frac{F_{max}}{E_{system}}) \tag{3.4}$$

In this study the phase 1 and 2 displacements are found from the displacement curve during dynamic testing. Although the phase 1 could be based on a current crushed distance after a certain time in operation and phase two may be based on a limit which cause leakage-before-failure. The system stiffness (E_{system}) is acquired through static tests at certain intervals during the dynamic testing.

When the remaining cycles is known, the lifetime can be estimated based on Equation 3.5 and a crushing rate (CR). This rate is found through a curve fit of phase 2 which was shown in Figure 2.6. It is worth to notice that the sample is supposed to fail when it reaches the end of phase 2. Hence, it should be conservative as it the remaining life in phase 3 is not considered.

$$Lifetime = \frac{l_{crit}}{CR} \tag{3.5}$$

3.2.2 Basic crushing rate

Based on several tests, the Figure 2.6 is a good representation of the displacement versus number of cycles for the composite. In order to quantify this behavior, it can either be attempted to curve fit the entire curve or just the linear section. The entire curve may be fitted with a function of the type logit, or the inverse of the sigmoid logistic function, see Eq. 5.8. The equation is shown without any added material or system constants. While the linear section should simply be fitted with a function of the type shown in Eq. 3.7. Either one of these equations can be used in combination with the data collected with regards to the S-N curves. The equations will be considered as the crushing rate.

Finally, it should be possible to predict either when the system will fail completely or when it will begin to leak, based on a given critical displacement.

$$f(x) = log(\frac{x}{1-x}) \tag{3.6}$$

$$f(x) = A + Bx \tag{3.7}$$

3.3 Actual crushed distance

The displacement measurements acquired through testing, also known as the cross head displacement, is measured through a LVDT in the tensile test machine This means that the displacement in the sample is potentially smaller than what is shown. It is desired to use an external LVDT ($LVDT_e$) in order to evaluate the relationship between the values from the attached LVDT and the cross head displacement (D_{ch}). When the displacement of the tube has been established, it can be assumed that the distance is due to crushing, main strain in the tube and strain in the hole area. Potentially the actually crushed displacement can be calculated by finding a ratio between the measurements from the external and internal LVDT (Eq. 3.8.

$$Ratio, R = \frac{D_{ch}}{LVDT_e} \tag{3.8}$$

The ratio will be evaluated for different loads and samples. Then for each sample, the actual displacement may be estimated by Equation 3.9.

$$D_{actual} = LVDT_e * R - \epsilon_{middle} * L \tag{3.9}$$

Where ϵ_{middle} is the longitudinal strain the middle of the tube and L is the initial distance between the top of the upper hole and the bottom of the lower hole.

3.4 Numerical Model

A simple numerical model is created in order to verify the measured strain distributions. The numerical model is based on work by Pederson (2008) and Skaar (2015) and supervision by Nils Petter Vedvik. The model and analysis were performed in ABAQUS/CAE 6.14-1. The model is 1/8 of the entire part. It z-symmetry was used when splitting it in half in the longitudinal direction and symmetry theta-symmetry was used when dividing the remaining model by four. The load was applied to the bolts as displacement control in the longitudinal direction. Material properties, such as Hashin Damage strengths and engineering constants was acquired from previous studies (Skaar, 2015) and (Perillo, 2014).

The following specifications were used when modelling.

Tube   In order to achieve more realistic results, it was decided to model the tube as a deformable solid. This was chosen because of the out-of-plane loads which will be generated. The part was meshed with hex-shaped structural elements.

Bolts   The bolts were modelled as discrete rigid shell elements. The part was meshed with quadratic structural elements. Each bolt was coupled to their own reference point as a rigid body.

Bolt-tube interaction   The surface-to-surface interaction were modelled with the bolts as master surface and parts of the tube as slave surface. Friction between the surfaces was formulated as penalty with a value of 0.2. Surface smoothing was enabled. It was decided to use finite sliding as it was more relevant in case of a progressive analysis.

A finite element model which properly simulates failure propagation is difficult and time consuming to create. This model was created in order to validate subjective hypotheses regarding strain distribution in the tested samples. Figure 3.1 shows the final model consisting of four parts - three bolts and 1/20 of the tube.
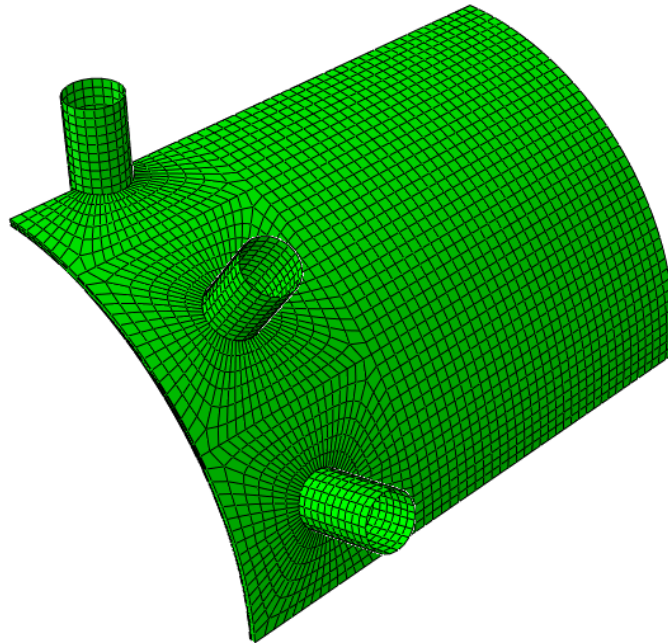
Figure 3.1: Finite element model of the given system.

Chapter 4

Experiment

All activity with regards to this thesis took place at IPM, NTNU Trondheim.

4.1   Materials

The system consists of an end fitting, a set of bolts, washers and bushings and a composite tube. The tube which is of most importance to this study was made out of glass fiber reinforced epoxy. Please see Appendix B for a more detailed description of the materials used when producing the composite tube.

4.2   Production and preparation of samples

All the tubes used in this study was created as a part of the preliminary studies (Horn, 2015). The procedure and other information regarding the produced tubes is still included in this thesis in order to ensure proper exchange of experience. The preparation may be divided into three stages: filament winding (Fig. 4.1), machining (Fig. 4.2) and sensor mounting. The following section will give a brief explanation of the three stages.

4.2.1   Filament winding

The production of the composite laminate tubes is based on the work of Dons (Dons, 2013) and Fosså (Fosså, 2014). This tube design involves the use of fiber mats in the bolt area of a

filament winded tube. It is referred to Dons' master thesis for further details. However, some improvements have been made by Fosså.

All tools and facilities necessary for this process was found in the composite lab, the plastic lab and the fatigue lab at IPM, NTNU. The filament winding was carried out with a four axed CNC winding machine, see Appendix C for full setup and material information.

Figure 4.1: Filament winding of a two meter long tube on steel mandrel. The structure to the far left is the curing oven.

The filament winding process necessary to produce the desired tubes for this study is relatively complicated. Because of the interface with the end fitting and the usage area for the final product the optimal layup is not the most convenient for filament winding. The layup, determined by Dons (Dons, 2013), is shown in Table 4.1.

The [0/45/-45] layers are applied as fiber mats. In previous work it has been recommended to wet the mats through vacuum infusion. It was decided to wet the mats through hand layup because the epoxy shall not cure under vacuum and the mats will be handled relatively rough when placed around the tube. An improved solution with regards to speed and Vf could potentially be to use prepreg.

The winding process went as following. After each hoop layer, the outer diameter was measured and the width of the mat was cut thereafter. The mats were wetted and placed onto the

Table 4.1: Production procedure by lay-up

Ply nr.	Fiber angles [deg]	Method	Joint placement, deg	Fiber tension
1	[90]	FW	-	15 N
2-4	[-45/45/0]	mat	0	
5	[+-12.7]	FW	-	15 N
6-8	[0/45/-45]	mat	90	
9	[90]	FW	-	35 N
10-12	[0/45/-45]	mat	180	
13	[90]	FW	-	35 N
14-16	[0/45/-45]	mat	270	
17	[90]	FW	-	35 N

mandrel. Then the fiber tension was adjusted according to specifications. Throughout the winding process the excess epoxy was wiped off by using a squeegee. When the winding was completed, peel ply was wrapped around the sample. The peel ply was used to create a flat surface over the entire tube, which is beneficial when placing sensors onto the tube. Thereafter the mandrel was rotated at a slow pace for twenty-four hours to avoid an uneven redistribution of epoxy during curing. The epoxy was completely cured after being rotated in an oven for 15 hours at 80 C.

When using a polyethylene mandrel, it is rather simple to pull the tube of the mandrel because the polymer will shrink inside the oven. A steel mandrel on the other hand will not act likewise and there will be a high friction between the GFRE and the steel. The problem is solved by applying release wax onto the steel pipe. The composite tube can then be removed by pulling the steel pipe out of the sample by using a jig, a chain hoist and an end-fitting. When pulled out, the tube is ready for machining.

4.2.2 Machining

The purpose of this step is to make the samples of the tube compatible with the test apparatus and the end fittings. It is a step that requires a high degree of accuracy. Any imbalance in the process may cause the bolt holes in the tube to not be concentric with the bolt holes in the end fitting. This may result in uneven loading of the tube during testing. A couple different procedures were tested throughout this study. All tools and facilities needed for these procedures are

found in the Realization Lab at IPM, NTNU.
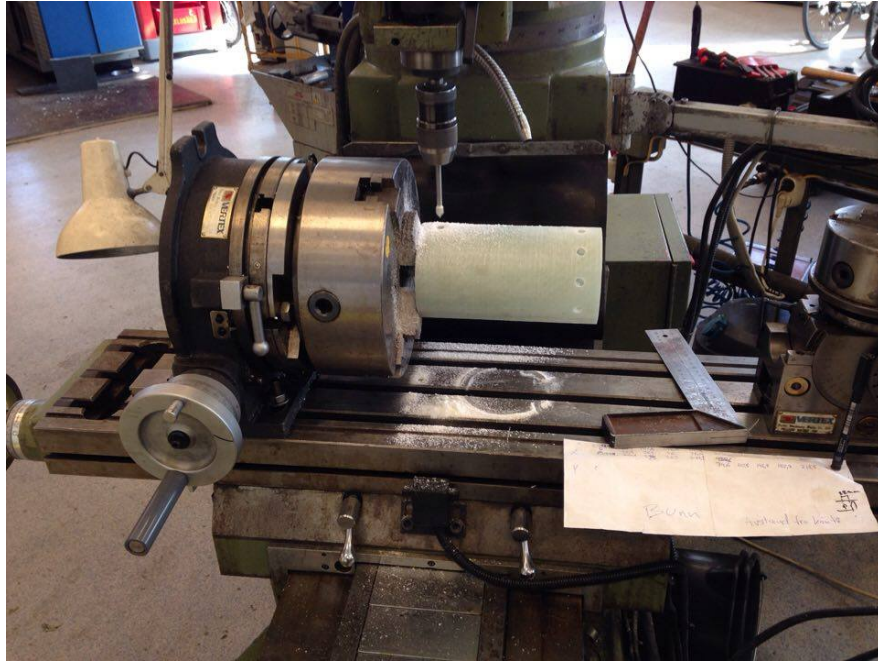
Figure 4.2: Machining of a sample in a three axis milling machine. The sample is locked into a rotary table.

The process involves cutting out samples at desired lengths, drilling holes which shall be concentric with the holes in the end fitting, and finally reaming the holes. The full process is more thoroughly explained Appendix C. The tools and machinery used is shown in Appendix B.

4.2.3   Bolts and bushings

In order to fasten the composite tube to the metal end fitting, bolts were used. The bolts are only subjected to shear load; by which they were held in place through two slots. In the interface between the bolts and the composite tube bushings made from a softer metal were used. The bushing (SKF PCM 081008E) has an outer diameter of 10 mm and inner diameter of 8 mm. The modified M12 bolts which were handed down from previous projects were used for most of the tests. At a later stage in the project, the bolt design was improved by shortening the machined distance. This will improve the assembly process by ensuring that the bushings are kept in the correct position and that the bolts cannnot be used to deform the metal end fitting. The old and new bolt design is shown in Figure 4.3.

Figure 4.3: Old modified bolt (left) and new modified bolt (right). The difference is the distance the bolts have been machined in the z-direction. The diameter of the machined area is 7.9 mm on both bolts.

4.3 Testing

4.3.1 Fiber volume fraction- Burn-off test

The fiber volume fraction (V_f) of the produced laminates is found through a burn-off test. The burn off test is conducted in order to establish the volume fraction (Vf) of each produced tube. This is necessary in order to evaluate the quality of the sample. It is also important when attempting to reproduce the results through similar tests or when comparing results with other studies.

The samples for the test shall be cut off from different locations in the respective tube. This will give an overview of the V_f at the respective location, as well as an average V_f. The samples are placed in ceramic cups which are then weighted before they are placed in an oven (Figure 4.4. In order to burn off the epoxy the samples must be heated in an oven for approximately 5 hours at 550 C. When the burn-off is complete, the cups which contain fibers are weighted. The weight data for the laminate and fibers is combined with density data of fibers and matrix in Equation 4.1 in order to find the fiber volume fraction

$$V_f = \frac{\frac{m_f}{\rho_f}}{\frac{m_f}{\rho_f} + \frac{m_e}{\rho_e}} \tag{4.1}$$

Figure 4.4: First burn-off test, accompanied with end fittings used in the filament winding process.

4.3.2 Static testing

An overview of the test setup can be found in Appendix B.

It is desired to establish the strength and the stiffness of the laminated tube in order make the results from this study reproducible. The sample will be statically tested in tension. The test will be performed at constant displacement. The displacement rate is 0.01 mm/sec. The displacement rate (DR) is chosen in order to enable comparison with previous studies. Regarding the effect of the DR on the results, it has been shown by Samborsky et al. (2009) that a lower displacement rate results in a lower tensile strength. Based on the respective study it is therefore assumed that the tensile strength results will be conservative. The test will run until a failure criterion is reached. In this study the failure is complete failure, which is chosen in order to gather as much data regarding the fatigue life cycle of the system as possible.

4.3.3 Dynamic testing

Figure 4.5 shows a fully sensor equipped sample ready for dynamic testing.

Figure 4.5: Sample, fully equipped with sensors.

The yield stress for the composite will be determined from the static tensile testing. The highest dynamic load (F_{max}) will be set as a fraction of the yield stress. The minimum load will be determined based on a R-ratio of 0.1.

$$R = \frac{\sigma_{min}}{\sigma_{max}} = 0.1 \tag{4.2}$$

The loading scheme is based on previous work, and the desire to create an S-N graph for the respective layup, material and geometry. The tensile fatigue shall be induced through a sinusoidal waveform with constant load amplitude. According to Dr. Echtermeyer, it is advised to run fatigue tests with a maximum frequency of 4 Hz in order to minimize temperature effects. In order to additionally run the tests efficiently we chose to use 4 Hz. The loading will hold at the mean force (F_{mean}) after a certain set of cycles. The elastic moduli will be measured at certain intervals because it is desired to monitor the elastic properties of the sample throughout the experiment. It will be measured by applying a linearly increasing load up to F_{max} at a rate of 0.01 mm/s. The cycle can be seen in Fig. 4.6.
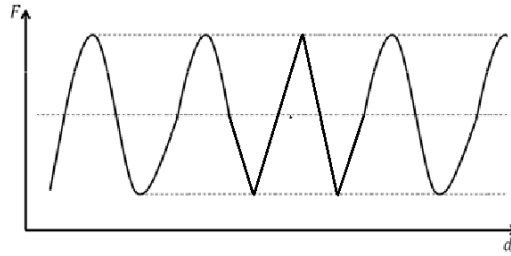
Figure 4.6: Graph showing the load cycle including the elastic modulus cycle used to determine the elastic modulus.

4.4 Sensor placement

LVDT   Because of limitations with the LVDT, it was only used when measuring the stiffness during the dynamic testing. The LVDTs were aligned with the upper and lower holes in position number 1. The positioning of the short LVDT is shown in Figure 4.7. A photo of the long and short LVDT installed is shown in Figure 4.5.

Strain gauge   Using strain gauges is a simple way to evaluate the strain at a given point. In this study they were used to evaluate data from the LVDT measurements and OBR results. Hence, they were only placed at points relating to the position of other sensors. Whether they were placed in longitudinal or hoop direction was dependant on the respect LVDT or optical fiber.

OBR   The benefit of using an OBR interrogator and optical fibers is the enabled ability to evaluate strain over a distance of up to 70 meters. Therefore, the optical fibers were often placed in hoop and longitudinal direction on the same fiber. Early in the phase it was experienced that issues might have occurred when a fiber was overlapping itself or another fiber. On the samples used in the results section, the fibers were placed in a configuration at which it would not overlap. The hoop fibers was placed approximately 6 mm apart from each hole in order to not get in contact with the metal end fitting. Longitudinal fibers were normally placed between between two holes in order to measure the highest strain.
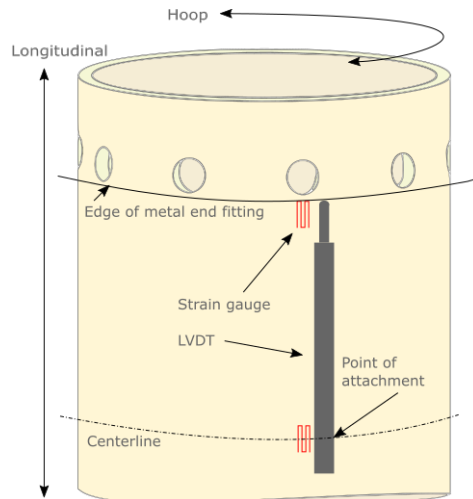
Figure 4.7: Position of strain gauges and LVDT on sample 4C.

4.4.1 Data acquisition

Several properties such as strain and displacement is of interest to acquire. The property data will be collected through internal sensors embedded in the tensile test machine and external sensors such as optical fibers, strain gauges and linear variable differential transformers. The embedded sensors show the applied load and the cross head displacement of the system. The external sensors are used to determine the local strain and displacement. The areas of interest are longitudinal strain at several points around the holes, and at the midpoint of the tube for reference. All the data is necessary in order to understand the actual behavior of the laminate when subjected to bearing loads, as well as the bolt connection system as a whole.

4.5 Quantity versus Quality

The experiment consists of three important factors. A complex sample/system to be tested. A wide range of sensor alternatives to be applied. Time consuming tests to conduct. All these factors contribute to a very time intensive process, especially when production and decommissioning is added. In order to avoid wasted time each test is evaluated before the next test is planned. This iterative process may compromise the quantity of tests which can be covered throughout the thesis. On the other hand, the risk of running a meaningless test will decrease and the quality of each test will increase.

Chapter 5

Results

The data presented in this chapter is based on results mainly from tests conducted as a part of this master thesis, but also the preliminary study.

5.1   Fiber volume fraction

The fiber volume fraction for produced tube four and five have been found through the master thesis work and the preliminary study (Horn, 2015). It is calculated with Equation 4.1. The data used in Equation 5.1 are based on results from the burn-off test for conducted for tube number four and data retrieved from Perillo (2014).

$$V_f = \frac{\frac{m_f}{\rho_f}}{\frac{m_f}{\rho_f} + \frac{m_e}{\rho_e}} = \frac{\frac{14{,}58g}{2{,}55g/cm^3}}{\frac{14{,}58g}{2{,}55g/cm^3} + \frac{5{,}96g}{1{,}19g/cm^3}} = 53{,}3 \tag{5.1}$$

Table 5.1 shows the volume fraction from tube four and five which were produced as part of the preliminary studies (Horn, 2015).

Table 5.1: Overview of volume fraction of the produced tubes

Sample #	4	5
Volume fraction [%]	53.3	58.5

5.2 Static testing

The focus of this study is to understand the behavior of the system during cyclic loading. In order to benchmark these tests to other tests, a static test is conducted for each tube which was made. This test will also contribute with fatigue data such as the maximum loading for a fatigue life of "one cycle".

Sample 4A and 4E were subjected to static tensile loading in the tensile test machine, see Appendix B for more info on the test setup. For 4E the test was ended at the point at which complete failure occurred, the complete cycle is shown in Figure 5.1. The test parameters can be found in Appendix E and F.
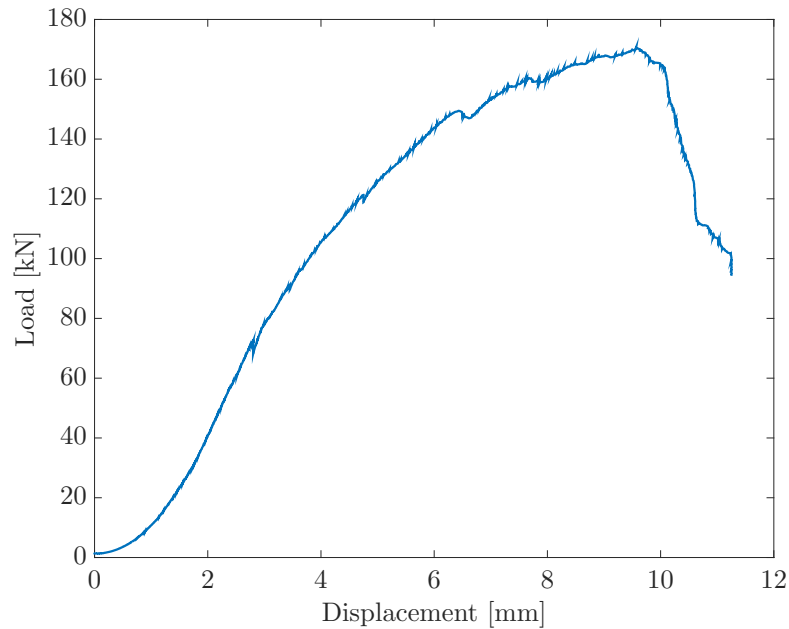
Figure 5.1: Load - displacement curve from the static test of sample 4E1

The load-displacement curve starts out steep, but has a gradually decreasing load-displacement rate. This may be due to matrix cracking, delaminations and deformation around the holes. These factors may contribute to strain softening by decreasing the stiffness of the laminate and varying the notch effect. It can be seen from the equation for the notch effect from elliptic notches (Eq. 5.2 that the notch effect will increase, hence there will be a strain softening.

$$K_t = 1 + 2 * \frac{b}{a} \tag{5.2}$$

In Eq. 5.2, a and b represents the radius in the load direction and transverse to the load direction, respectively.

Further on, a pop in occurs at 149.4 kN load and 6.43 mm displacement. It is assumed that at this load, fiber fracture occurred. The section between the pop in and maximum load is assumed to be governed by crushing of the laminate through fiber fracture, splitting and kinking. The ultimate force and displacement was 170.9 kN and 9.57 mm, at this load the sample failed through shear out.

Data regarding the ultimate tensile strength, load at which strain softening becomes significant and the critical load for an e/d-ratio of 2.2 was established as a result of running the test until failure.

5.3   Dynamic testing

The main goal for this study is to establish an S-N curve for the system during cyclic tensile loading with an R-ratio of 0,1. Additionally, a set of other parameters are analyzed in order to have the ability to quantify the lifetime of specimens subjected to different loadings. All curve fits have been generated through the use of Matlab's Curve Fitting Toolbox™, which utilizes the least squares fitting method.

An important remark is the jumps which can be noticed in Figure 5.2. At first the jumps were thought to be caused by shear out at single holes due to uneven loading. After the final test it was noticed that the piston in the machine was inclined. It appeared that out of the ten bolts used to hold the upper and lower part of the piston together, ten had failed. Although there is no clear evidence to what the cause of the jumps was, it was decided to continue the analysis by assuming that the jumps were occurred every time a bolt failed. This assumption is based on several arguments which are further explained in the Appendix G.
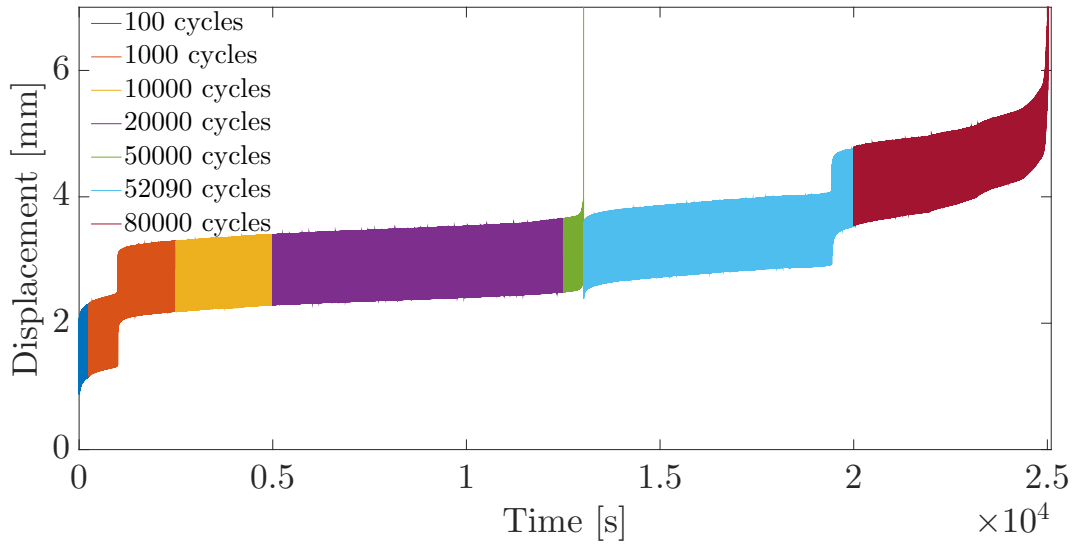
Figure 5.2: Displacement during cyclic loading (raw data with jump) - 5A

The dynamic results logged at 50 Hz can be seen in Figure 5.2 where the cross head displacement has been plotted against time. In Figure 5.3 the results from the stiffness tests during the dynamic testing is shown. The results from all tests have been processed and the results can be seen in Figure 5.4. In this figure the plot resembles the maximum load at a given cycle.
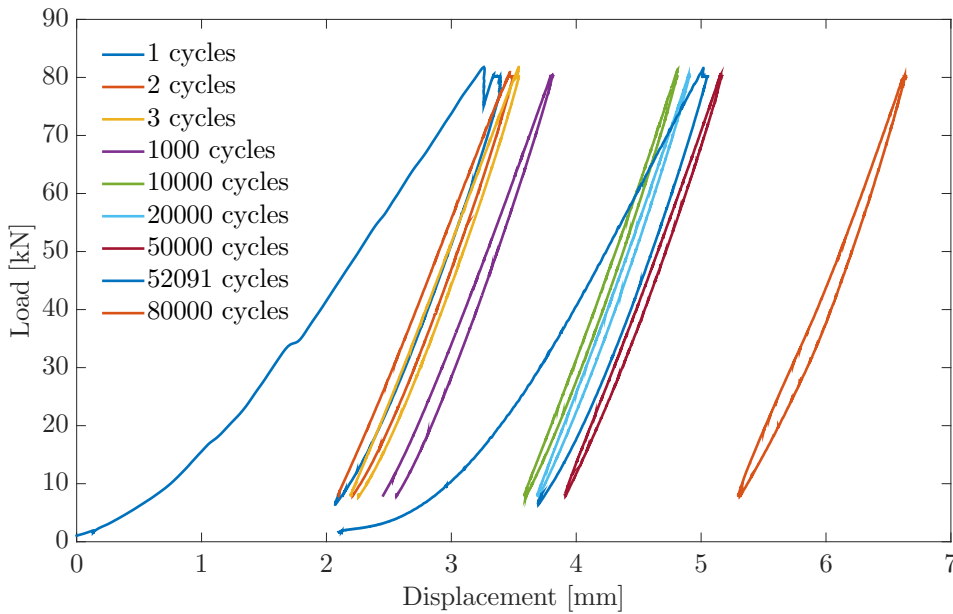
Figure 5.3: Displacement-loading curves after n cycles - 5A
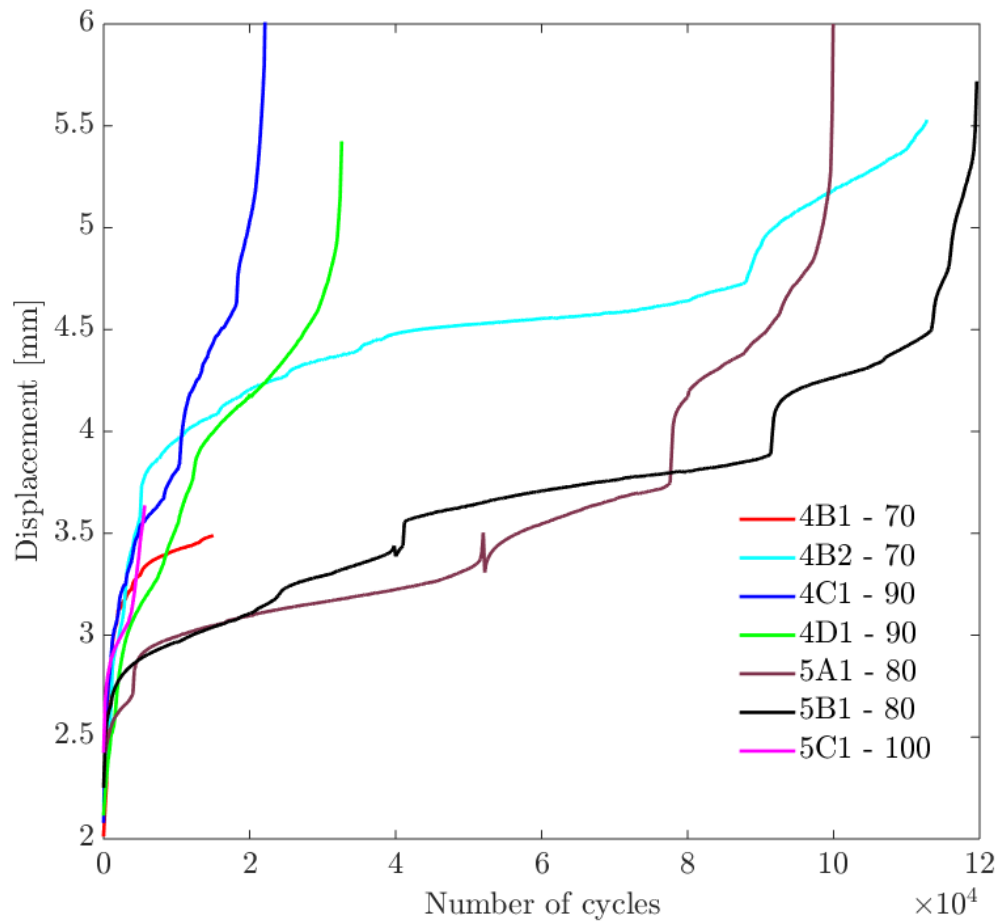
Figure 5.4: Maximum displacement for all tests throughout the respective life times.

5.3.1   S-N and S-D curves

In this section a set of curves are displayed. Normally S-N curves are shown with stress on the y-axis and number of cycles on the x-axis. The sample which is studied in this thesis does not have the same cross section all over in the tube. For a standard sample it would be natural to use the smallest cross section in order to estimate the stress based on the applied load. For this work it has been chosen to plot the amount of cycles against the applied load. Calculating the highest nominal stress would be a complicated estimate due to factors such as notch effects and surface effects. In addition, evaluating based on the applied load will be more applicable when comparing to industrial applications. Hence, the S-N and S-D curves does not use the applied

stress, but the applied load.

Both curves are based on six tests, with a maximum load of 80 kN (two tests), 90 kN (two tests), 100 kN (one test) and the static test which failed at up to 170 kN. The dynamic tests had an R-ratio = 0.1. The Figure 5.5 consists of three plots which describes the amount of cycles until three different types of failures for different loads. The failure modes are shear out / ultimate failure, critical point at which the displacement escalates just before ultimate failure and leakage before failure. Leakage before failure is defined as a displacement of four millimeters, which is when the bolt hole reaches the o-ring. The Wohler curve is explored through three different curve fits. These lines were found through the Matlab curve fit tool - *cftool*. A power law fit (Eq. 3.1), a log-log fit (Eq. 3.2 and a semi-log fit (Eq. 3.3) were used. The power law fit was advised by Samborsky et al. (2009) and proved to give a good fit for values over 1000 cycles with an adjusted R-square value of 0.977. The DNV advised log-log curve fit was a bit worse with an adjusted R-square value of 0.958. The best fit for the fatigue life above 1000 cycles was the semi-logarithmic curve fit with an adjusted R-square value of 0.982.

In order to show how a S-N curve may be created based on a certain threshold, another curve was created. The critical limit, e.g. leakage-before-failure is considered as a displacement of 3.3 mm. The values were curve fitted with a semi-log curve fit for comparison. The quality of the curve fit was low, with an adjusted R-square value of 0.64. This is mainly because the results for 100 and 90 kN were in the same range.
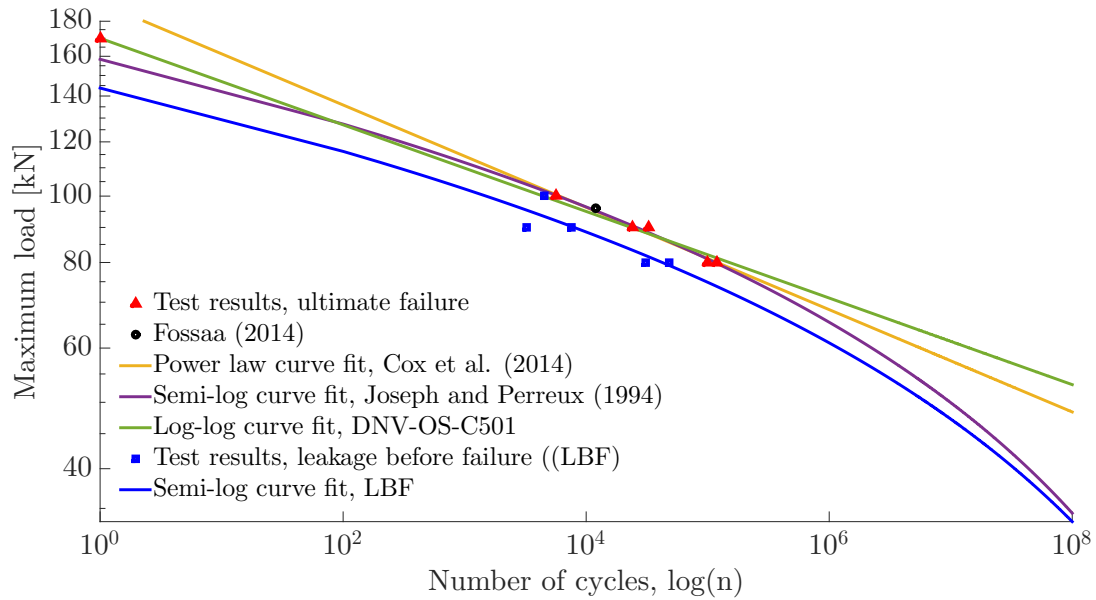
Figure 5.5: S-N curve | R=0.1

In addition to the S-N curve, a S-D scatter plot has also been created. See Figure 5.6. As mentioned in the model section, the S-D curve is necessary in order to fulfill the given models. It can be seen in the plot that the displacement at 80 and 90 kN is very similar to each other, but much larger than for 100 kN. It is expected that the crushed distance will become larger with larger smaller loads, as this results in a lower critical e/d-ratio. However it is interesting to notice how similar the displacement is for the tests ran at 80 and 90 kN max load. The coinciding displacement, which ranges between 5.57 mm and 5.8 may be important when attempting to model and predict the same system subjected to different loads.
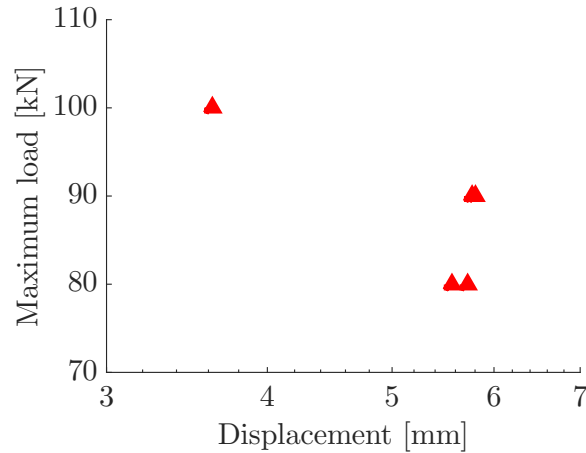
Figure 5.6: S-D curve

5.3.2 Stiffness based model

Based on the residual stiffness model explained in the chapter "Model" we the S-N curve data and the stiffness and crushing rate at maximum load in order to evaluate the lifetime. Creep effects are of importance when using results from static tests and dynamic tests in the same model. This is further explained in the chapter "Discussion".

5.3.3 Phase 1 - displacement

The overall displacement in phase 1 is considered to be the displacement needed for the system to stabilize. In other words, the displacement until a relatively uniform crushing rate occurs. This displacement is reached when the crushing rate is 105% of the phase 2 displacement rate. For example, this value is at approximately 2.85 mm for the samples subjected to a maximum load of 80 kN.

Phase 2 - Stiffness

Stiffness over time   The dynamic tests were paused after different intervals in order to measure the stiffness and maximum displacement. The procedure is explained in chapter 4 - Experiment. The results from the different samples can be seen in Fig. 5.7 and the raw data curves from sample 4B1 can be seen in Fig. 5.3. It is apparent that the stiffness does not change substantially

within the load interval which is evaluated, except during the first five cycles. This was first measured in order to evaluate whether the residual stiffness may be used for failure prediction. At a later stage it is evident that the failure stiffness may be used for estimating the allowed displacement at a given load scenario. Although the elastic modulus is relatively static there is a substantial difference between the different samples.
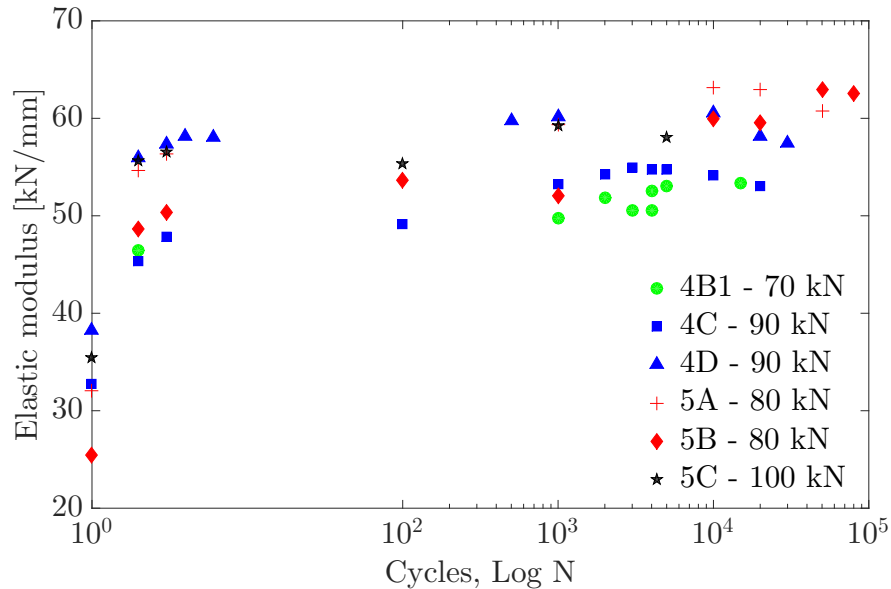
Figure 5.7: Elastic modulus after n cycles for different samples and cycles. The average elastic modulus for loads above 50 kN of sample 4B1, 4C, 4D, 5A, 5B and 5C is shown.

Global stiffness For samples the stiffness appears to vary between approximately 50-63 kN/mm for the majority of the lifetime. The variations are smaller for samples tested at similar loads. At 70 kN max load the stiffness was between 50-53 kN/mm. Then it increased to 59.5-63 kN/mm with 80 kN max load. At 90 kN the span was larger and was between 53-60.5 kN. Finally, for the one sample ran with 100 kN max load, the span ranged between 58-59 kN for the majority of the life time. Based on these observations we can conclude that the stiffness used in a potential model is dependent on the applied load.

Position at maximum load - displacement rate

From the stiffness tests conducted during the dynamic testing, the displacement at maximum load was logged. These data points have been plotted and linearly curve fitted, see Figure 5.8. It

is apparent that the results are quiet similar as with the global stiffness. The rate is quiet similar for the same load scenarios, but differs between different scenarios. The difference from the global stiffness is that the displacement rate does increase with increasing maximum applied load, which is expected. The slopes for all curve fits are found in table 5.2
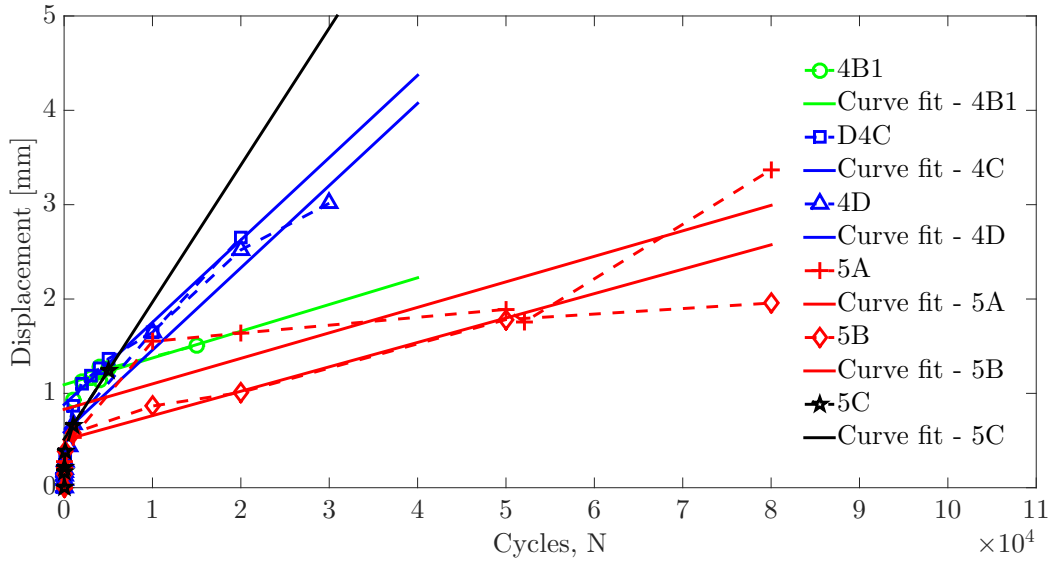
Figure 5.8: Linear curve fit for the displacement at maximum load after n cycles.

Table 5.2: Slopes for each linear curve fit as shown in Figure 5.8.

Sample	4B1	4C	4D	5A	5B	5C
Slope [mm/cycle]	2.83e-5	8.73e-5	8,72e-5	2.7e-5	2.59e-5	1.45e-4

Complete model

An example for the complete model is created based on data from 4D. The critical number of cycles until failure is "estimated" to 29400 with a maximum displacement of 4.6 mm. The stiffness is approximately 55 kN/mm and the displacement rate is 8.725e-05 mm/cycle. The displacement after initiation phase at zero load is approximately 1.19 mm. Figure 5.9 shows the different variables.

$$Critical\ length = d_{ph2} - \frac{F_{max}}{slope} - d_{ph1} = 4.6mm - \frac{90kN}{55\frac{kN}{mm}} - 1.19 = 1.77mm \qquad (5.3)$$

$$Lifetime = \frac{1,77mm}{8.725 * 10^{-5}\frac{mm}{cycle}} = 20328 \; cycles \tag{5.4}$$

At this point the model appears to be slightly radical, as the analysis results in 20328 cycles and expected value based on the experiments should be 19596 cycles. It should be mentioned that the two displacements which were used can be varied depending on the system and applied loads. The only criterion is that the two points must lie within phase 2. As of now, the model seemed relatively correct. When used properly it would instead use mean values from several tests in order to evaluate the remaining life time of a separate scenario.
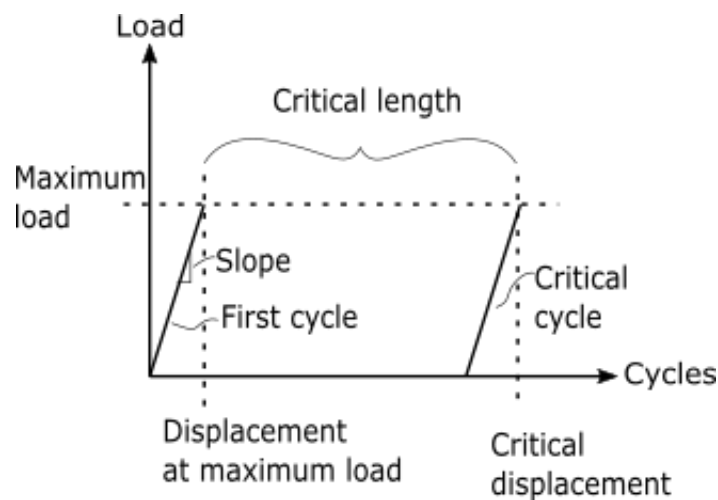
Figure 5.9: The different variables included in the fatigue modulus model.

Original fatigue modulus model

An attempt to use the theory behind a fatigue modulus has been attempted. In theory, it not directly transferable to the studied system, because of the introduced stress concentrations due to bolt connections. Nevertheless, it is a model which incorporates the ratio of applied stress to the strength, maximum strain and potentially stiffness over time.

The results from sample 4B1, 4C, 4D, 5A, 5B and 5C is shown in Figure 5.10. It is apparent that every graph behaves differently, but a trend towards exponential decay at the end of the life time is apparent. The magnitudes also vary remarkably. Either way, the appearance of a trend means that there is something to build on. This supports the original use of a fatigue modulus as a variable which can be used for fatigue modelling.
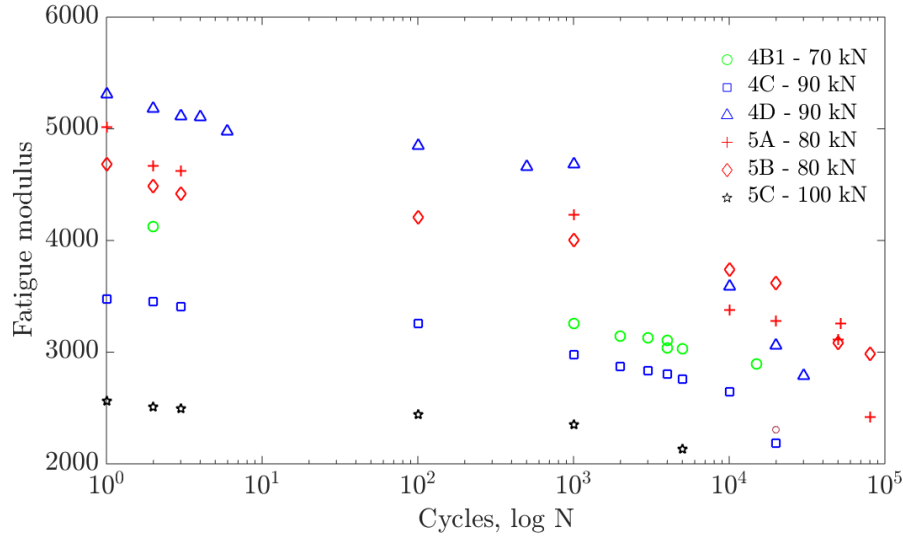
Figure 5.10: Fatigue modulus over the lifetime for different samples.

5.3.4 Displacement per cycle

Figure 5.4 shows a summary of all tests. The lifetime of the tube can be split up into three phases: the initiation, steady crushing and failure. In the same figure it can be seen that the initiation process ends at approximately 500 cycles for all samples. The crushing rate is remarkably higher in phase one compared to phase two. Then when a critical limit is reached phase 3 begins.

The crack/crush propagation has been calculated for intervals of approximately 4 cycles at a time in order to properly estimate the average values and phase limits. Table 5.3 shows the results for sample 4C. The crushing rate was calculated through the following steps: The variable c represents the displacement at the k'th measurement.

1. Average of values over 4 cycles

$$Average_{interval(k->k+49)} = \frac{c_k + c_{k+1} + ... + c_{k+49}}{50} \tag{5.5}$$

2. The slope between the average values of two neighbouring intervals

$$Crushing\,rate = \frac{Average_{int2} - Average_{int1}}{8} \tag{5.6}$$

3. The average value over a larger interval

$$Crushing\,rate = \frac{CR_1 + CR_2 + ...CR_n}{n} \tag{5.7}$$

Table 5.3 shows the crushing rate for sample 4C for the respective intervals. It is gradually reaching its lowest value when approaching 10000 cycles. By calculations it is evident that between 3000 and 20000 cycles the C.R. ranges between $0.5 * 10^{-4}$ and $1.1 * 10^{-4}$ mm/cycle. Those 17000 cycles represent approximately 70 % of the lifetime of the given test. By ignoring the two jumps between 10000 - 20000 cycles it is possible to get a fair estimate of the displacement after n cycles during phase 2.

Table 5.3: Crushing rate, sample 4C

Interval [cycles]	100-999	1000-1999	2000-2999	3000-3999	4000-4999	5000-9999	10000-19999	20000-23930
Crushing rate [mm/cycle]	3,24e-04	1,75e-04	1,34e-04	1,08e-04	1.09e-04	4,64e-05	9,36e-05	2,87e-04

When designing a system, it is essential to understand the minimum allowable crushed distance before shear out will occur. This is either to know where to place a possible barrier, such as leakage before failure. Additionally, it can be used to estimate the lifetime of the product.

Logit curve fit

The logit function, also known as the inverse of the sigmoidal logistic function can be seen in Equation 5.8. The logit function was modified to give a better curve fit, see Equation 5.9. C is a curve fit constant and N is the estimated lifetime given by the S-N curve. An example has been generated for 4D. By setting 32930 as N, a as 0.3549 and b as 214.7 which was achieved for a curve fit for 4D using *cftool* in Matlab. The result is shown in Figure 5.11. Based on this data we can estimate the remaining lifetime of a sample similar to 4D. If we assume that the critical displacement at mean load is 4 mm and the structure has been displaced 3 mm, then we can solve the function for x and find the values for x when y is 3 mm and 4 mm. The results are respectively 2520 cycles and 19090 cycles. Hence, the remaining lifetime is estimated to 16570 cycles. This turned out as a conservative estimate compared to sample 4D which would have had 11896 cycles left for the same interval. This was not conservative due to the model,

but rather because of the quality of the curve fit. Hence, it is completely arbitrary whether this estimate is conservative or radical. On the other hand, we are using a critical limit (in this case 4 mm) which makes the estimate conservative.

$$y = log\frac{x}{1-x} \tag{5.8}$$

$$y = a * ln\frac{x}{N-x} - a * ln\frac{b}{N-1} \tag{5.9}$$
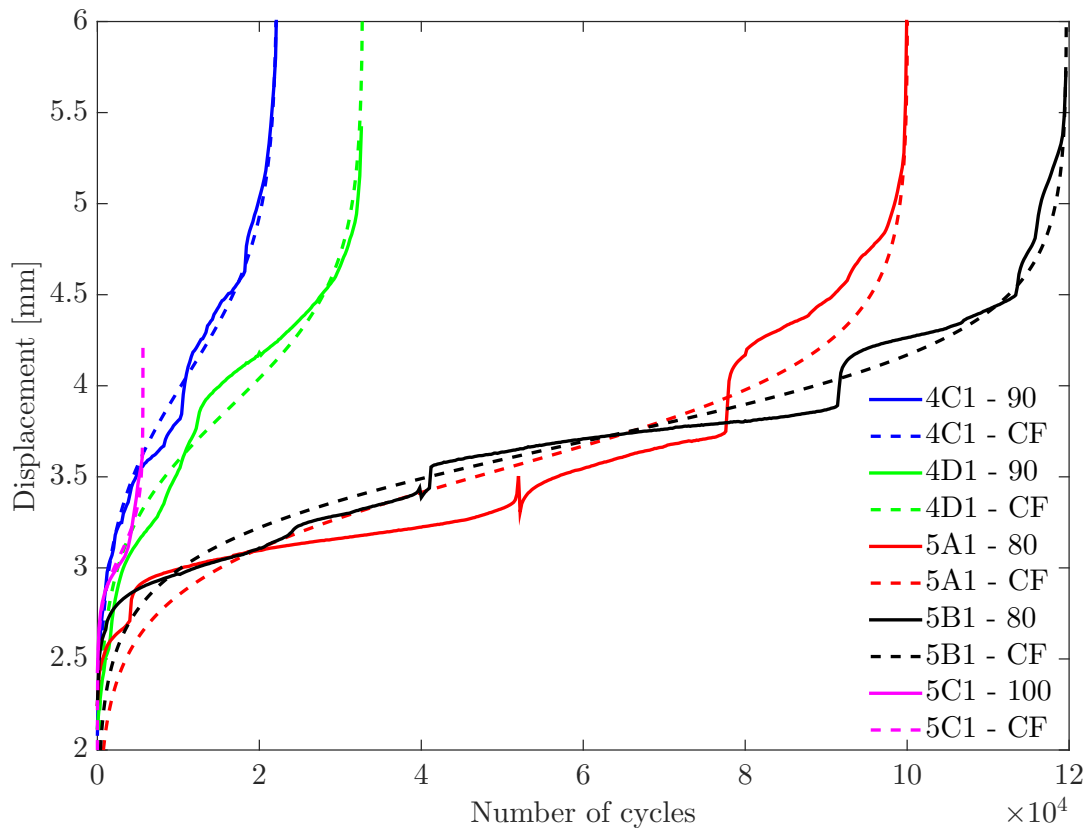
Figure 5.11: The average values over the dynamic testing combined with a curve fit based on the logit function.

5.4   Validation of test parameters

At the beginning of the dynamic testing there were some doubts regarding data sampling and the actual capabilities of the tensile test machine. First, the lowest possible sampling rate was evaluated. Theoretically it was estimated to be at 25 Hz, but practically it appeared to be 50 Hz.

The other issue was whether the system was capable of reaching the planned maximum and minimum loads with the planned frequency or vice versa. The maximum and minimum loads was simply monitored and verified on the Instron display, and appeared to be correct. The frequency was validated by analyzing one of the tests with a simple Matlab function used to find local maximums. Hence the tensile test machine appear to have worked as expected.

5.5   Actual displacement

In order to evaluate how the cross head displacement translates to the actual deformed or crushed distance, both strain gauges and linear variable differential transformers (LVDT, see the) were used. When testing sample, 4C two SGs and one LVDT were incorporated and when testing sample 4D two LVDTs were incorporated. The benefit of using LVDTs is that it makes it possible to measure the distance between to known points. The downside is that it does not measure the displacement on the entire circumference of the tube. Hence, if there are any variations, it will not be noticed.

Figure 5.12 shows results from an arbitrary static cycle from the test of sample 4D. The results which are compared is the displacement of the overall system and the displacement of the tube at one point on the perimeter. The results are from measurements from a LVDT mounted at the two metal end fittings and the cross head displacement. The displacement shown in the overall system is over 70% larger than the displacement shown at the point of measurement with the external LVDT. The variation in the difference between the cross head displacement and the LVDT measurements appears to vary linearly. The variation has been plotted for all cycles in Figure 5.13.
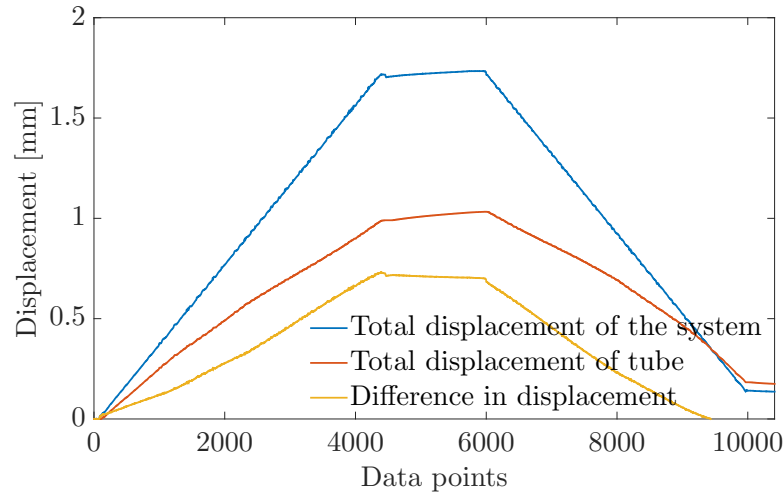
Figure 5.12: Example from an arbitrary cycle.
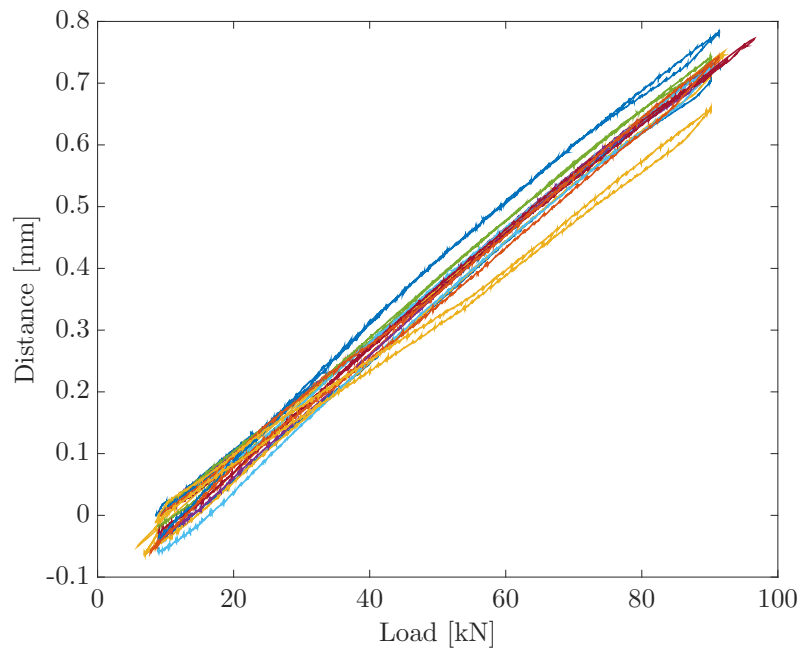
Figure 5.13: The variation between the difference in cross head displacement and the displacement measured by the LVDT. The results are shown relative to the applied load. These are results from static tests conducted on sample 4D during the dynamic testing.

The respective setup was also used to evaluate the differences between the displacement in the upper and lower part of the tube. For sample 4D it appeared that the displacement in the lower half of the tube was generally higher than the displacement in the upper half. The

difference increased slightly with the amount of cycles, but towards the final half of the lifetime the difference increased remarkably. The tube failed in the lower half.

From the test of sample 4C a comparison between the external LVDT and two strain gauges are shown in Figure 5.14. The positioning of the strain gauges and LVDT is shown in the chapter "Experiment". The cross head displacement is also taken into account. The LVDT had to be mounted before every test, which results in slightly different positioning every measurement. The graph showing the LVDT results therefore only shows the relative displacement for the respective cycle. The displacement relative to the previous cycle cannot be shown.
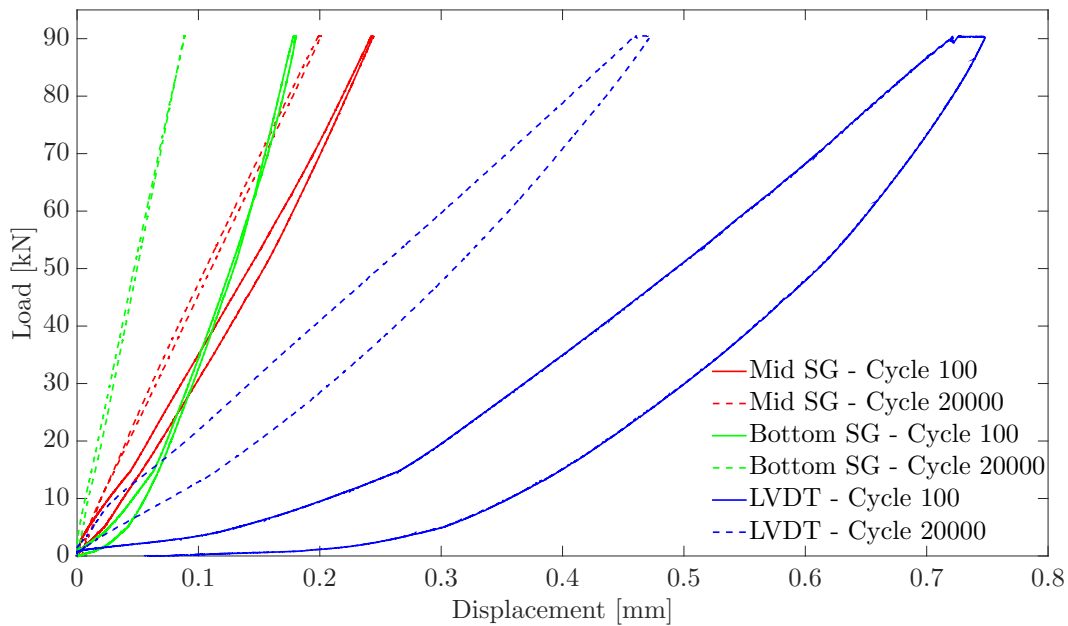
Figure 5.14: LVDT measurements compared with strain gauge measurements for the 100th and 20000nd cycle.

The displacement from the two SGs shown in Fig. 5.14 is a result of estimating the deformation by multiplying the strain from the strain gauges with the length of the distance measured through the LVDT (83 mm). The main finding from examining Figure 5.14 is that the displacement due to crushing/deformation in the area around the bottom holes is substantially larger than the displacement due to deformation of the uniform area of the tube. This will vary with the length of the tube, but for sample 4B1, 4C, 4D and 5A-C it is useful knowledge when evaluating the actual crushed distance.

By utilizing LVDTs during the dynamic testing of sample 4C and 4D it was found that the displacement of the tube relative to the displacement of the cross head displacement varies linearly. There are also apparent variations between the displaced distance of the upper and lower half of the tube. Previous tests have shown that bending occurs in the system, which means it can be assumed that the displacement also varies between every hole pair.

5.6   Failure types

The crushing behavior seen during testing can be described by a collection of several failure modes on micro level. Because the tube is connected to the tensile loading through bolts, it is subjected to both compressive and tensile loading depending on which area is inspected. Hence, the area around the hole is divided into three sections: the compressed area, the tensioned area and the middle area of the hole. The compressed area has been studied in a microscope. The samples were cut at the positions shown in Figure 5.15a and placed in an epoxy bath. The cured epoxy block (Fig. 5.15b) was sanded with 120, 240, 400, 1200 and 4000 grit sand paper. It was chosen to use microscopy in order to evaluate the failure modes at micro level.
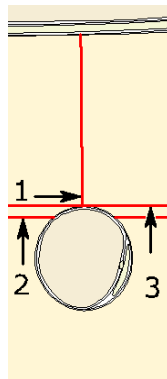
(a) Cut lines for cross section of microscopy views.   (b) Sanded epoxy block filled with samples.

The area below the hole sustains relatively low loads, as can be seen in Figure 5.16. On the other hand, it is the only area where it is possible to get close to the hole without being squeezed between the tube and the metal end fitting. It is therefore a plausible position for the SMH/OBR system, although this is not where critical failure will occur.
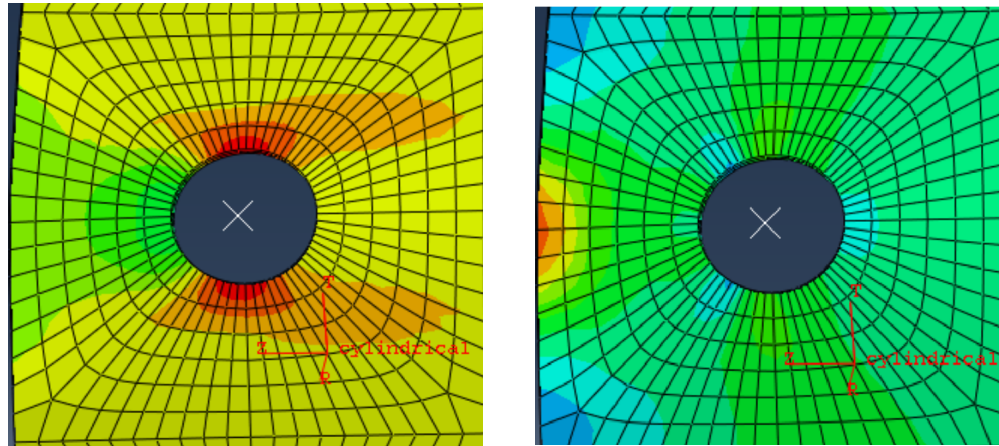
(a) Stresses in longitudinal direction, z-direction in the coordinate system. Green symbolise compression, while red symbolise tension.

(b) Stresses in hoop direction, theta-direction in the coordinate system. The color blue and red symbolises compression and tension, respectively.

Figure 5.16

The area at the middle of the hole will be subjected to the highest longitudinal stresses as well as shear stresses. High longitudinal loads in the 0 plies may cause fiber fracture and pull-out, while it may cause splitting in the 90 plies. The +-45 and +-12.5 layers are subject to both failures.

The above area is the area subjected to crushing. Fiber kinking is expected on the 0 plies, fiber fracture and/or splitting is expected on the hoop plies. While both may occur in the +-plies. The microscopy photo shown in figure 5.17 shows how kinking occurs in one of the middle 0 degree plies on the top edge of the hole.
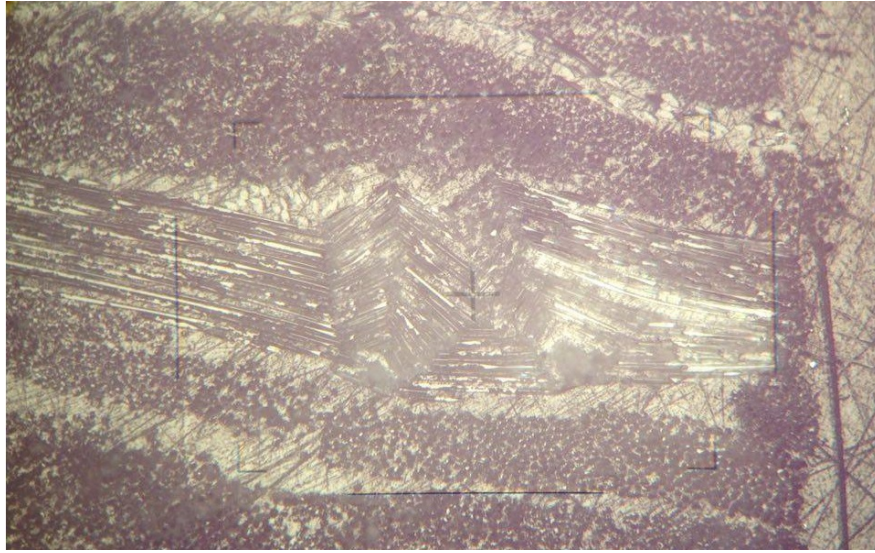
Figure 5.17: Fiber kinking seen through transverse view (position #1, fig. 5.15a) at 200x magnification through microscope.

Another possibly related effect occurs at the outer and inner face of the laminate. Figure 5.18 shows that delamination occurs between some of the laminae. The out-of-plane loads which cause the delamination could either be due to the free edge effect or a wedge effect. The free edge most be considered at the middle of the hole where the different laminae may have room to move. Because the outer layer has fibers located in a direction perpendicular to the load, the free edge effect will counteract delamination. Hence, the delamination probably occurs due to kinking of the 0 degree plies which cause a wedge effect.

Delamination is also occurring from the middle of the hole and up above the hole with a diameter of up to 10-15 mm. The cause of the delamination is most probably due to shear loads between plies 0 or 90 and +-45 plies.
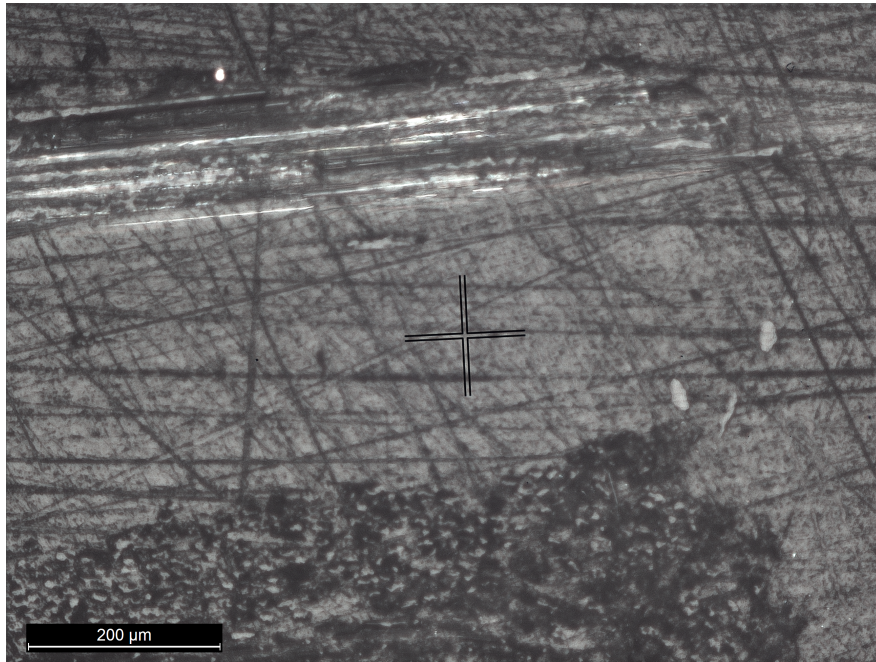
Figure 5.18: Delamination between the two outer plies, seen from the #2 cross section shown in Fig. 5.15a.

Ultimate failure has been established as shear out, which can be seen in Figure 5.19. Another secondary failure is also apparent, as both the outer and inner lamina have been separeted from the sample. These laminae were wounded in hoop.

Figure 5.19: Sample ultimately failed due to shear out.

5.7 Structural Health Monitoring

Strain has been measured with an optical backscatter reflectometer interrogator through the use of optical fibers. The fibers were placed on the surface of all of the samples, but only three of the tests showed usable results. Optical fibers applied to the outside of the sample can be rather fragile which is the reason why only a few results turned out as they were supposed to. Either the fibers broke during installation of the sample into the test jig, or during testing. Of the successful measurements, results from testing of sample 4E and 5C is presented.

Sample 4E was tested statically. Fibers were placed in hoop both 6 mm (opposite direction of the load) from the lower row of holes and 6 mm from the upper row of holes. Measurements from the static test is shown in Figure 5.20 and in Fig. 5.21. The first figure shows the overall measurement, and it can be seen that the strains in longitudinal direction is remarkably higher than those in hoop. It is also noticeable that the load distribution is relatively uneven, in the beginning, but evens out with increasing load. Although, at max load there is still a fairly uneven distribution.

A strain gauge was placed in hoop, next to the optical fibers above one of the holes. The SG measurements and OBR measurements have been represented together in Figure 5.21. It should be mentioned that the SG is placed further away from the hole than the optical fiber. Therefore, the strain is not expected to be the same. It can be seen in the figure that for higher loads, the SG measurements is generally lower than the OBR measurements, but they do follow the same pattern. It is expected that the OBR measurements show accurate strains, based on the article "Measuring changing strain fields in composites with Distributed Fiber-Optic Sensing using the optical backscatter reflectometer" by Grave et al. (2015).
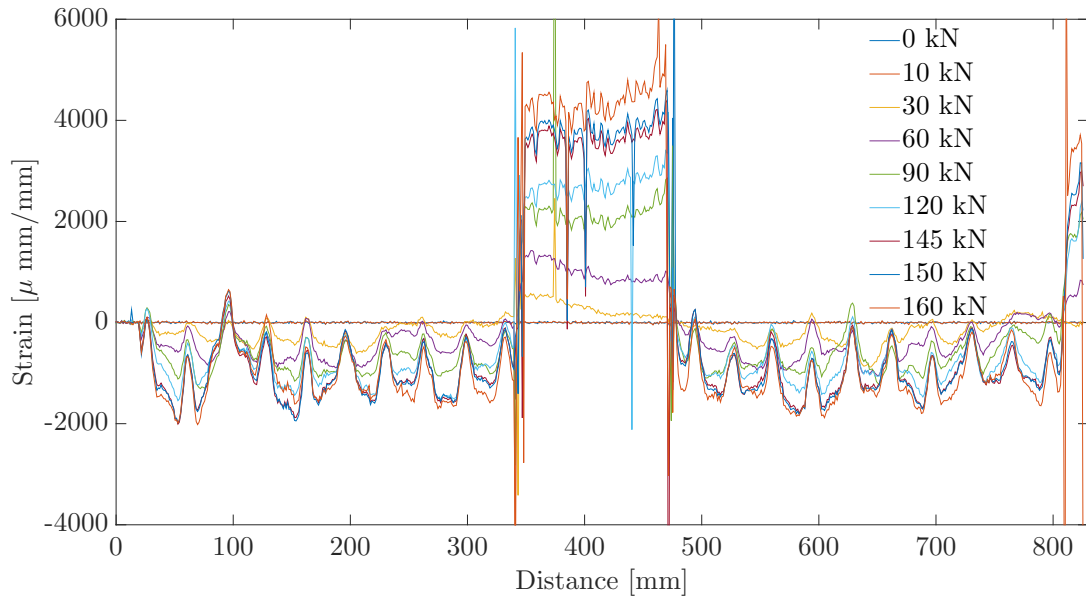
Figure 5.20: OBR measurements of sample 4E1. Left section is the lower hoop strain, mid section is the longitudinal strain and the right section is the upper hoop strain.
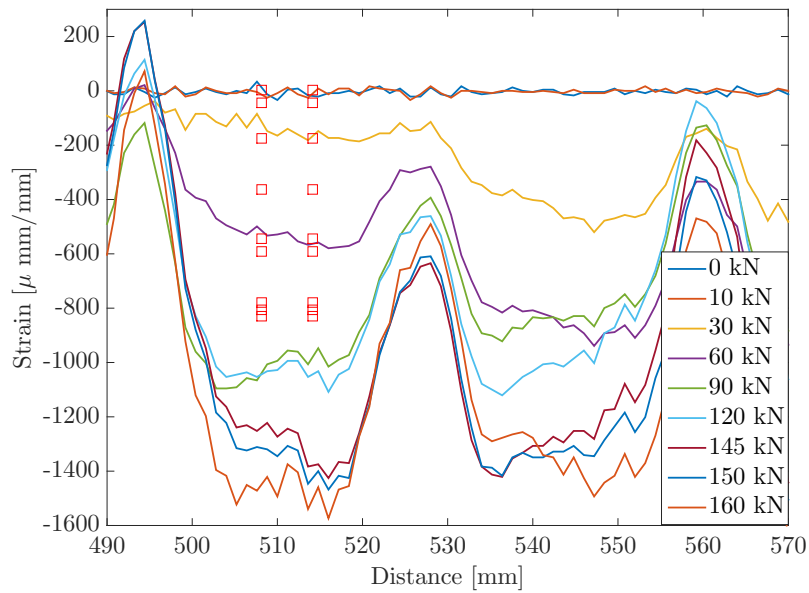
Figure 5.21: Strain gauge measurements compared to OBR measurements for sample 4E1. The red squares resemble the outer points of the area covered by the strain gauge. The SG covers 6 mm, while the OBR SG covers 2 mm.

The results found from the dynamic testing of sample 5C have been analyzed. The sample was instrumented with an optical fiber in hoop, both by the upper and lower row of holes.

Additionally, the optical fiber was placed in the longitudinal direction between eight out of ten hole sections. The longitudinal data has been processed and is presented in Figure 5.22. Three important findings are shown. First of all, the load distribution is uneven, but relatively static throughout the lifetime. Second, it is section dependent whether the largest strain is towards the top or the bottom of the tube. Third, the strain is largest at the section where the magnitude of the strain is equally large at the top and bottom.
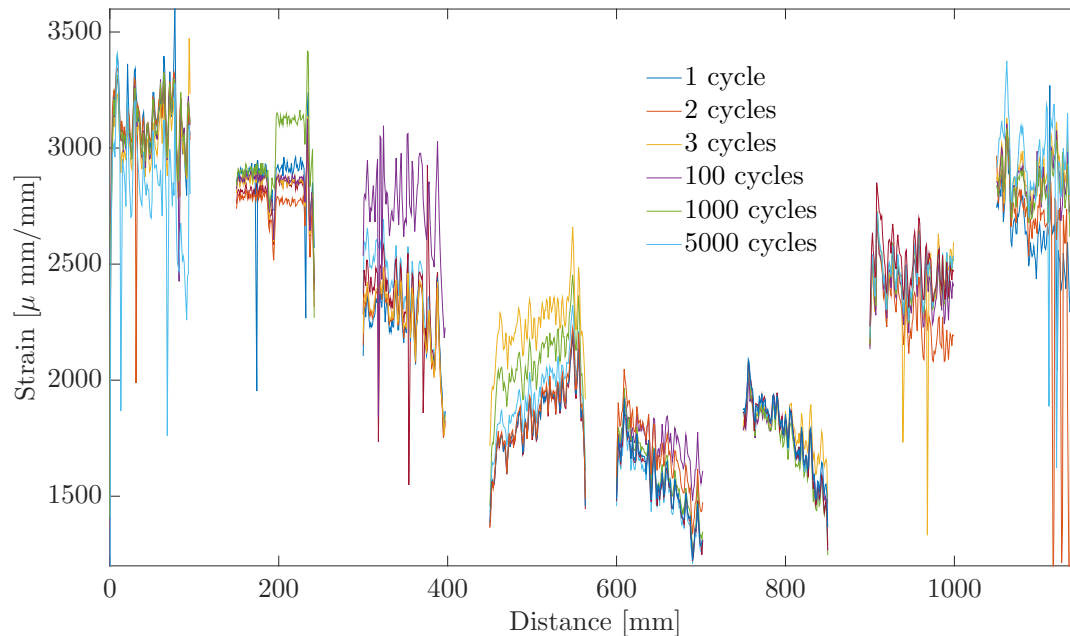
Figure 5.22: Longitudinal measurements of sample 5C at maximum load during dynamic testing. The direction from left to right in the plot resembles the direction from top to bottom in the tube.

Another way to acquire the same findings is by evaluating the hoop strain for the upper and lower row together. Figure 5.23 shows two graphs, where the upper graph shows the hoop strain in the upper row and the lower graphs shows the hoop strain in the lower row. The position to a hole is related to the points with highest compression (negative values). The highest peak, which is in tension, arises because a section of holes are not loaded. The sections with the highest compressive loads is also the sections with the highest tensile loads in Fig. 5.22. The same behaviors which were seen in this figure can also be seen in figure 5.24. Here, one measurement from the upper and lower cycle has been placed together. It is noticeable that especially one hole in the bottom row is carrying a large fraction of the load. Additionally, the load distribution
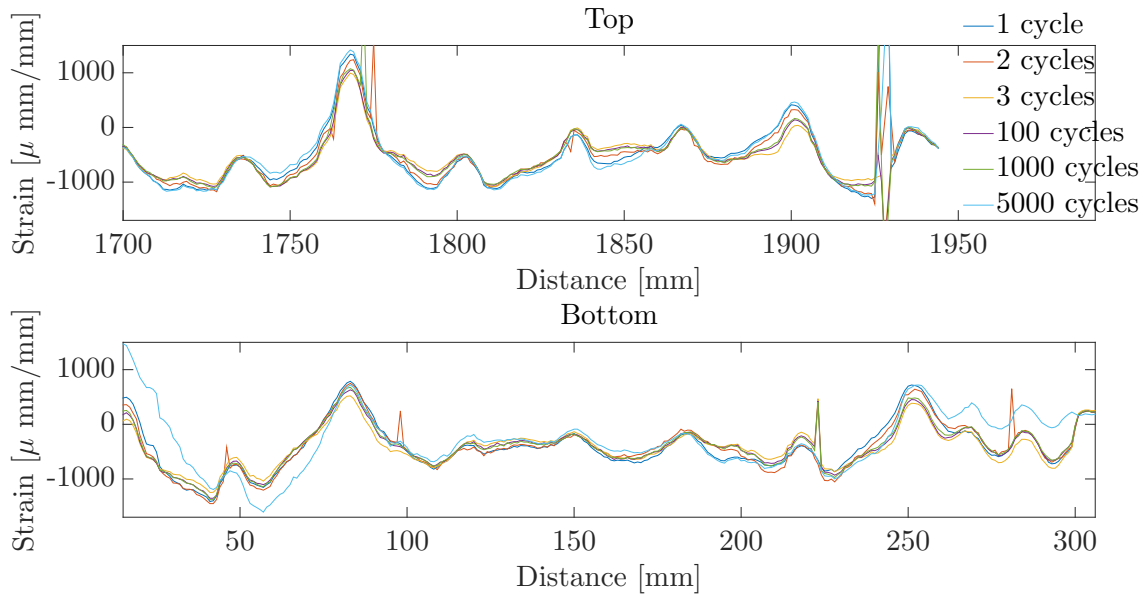
Figure 5.23: Comparison between the OBR measurements in hoop near the upper and lower row of holes. The measurements are retrieved from the dynamic test of sample 5C.

in the bottom row follows the same distribution as the one shown in 5.22.
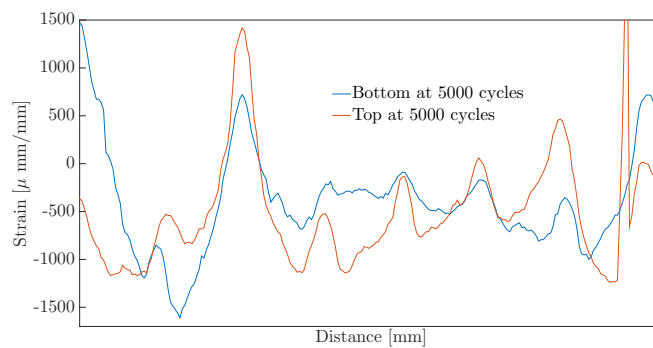
Figure 5.24: The hoop strain in the top an bottom at 5000 cycles.

Chapter 6

Discussion

S-N curves

The S-N and S-D curves have been established based on six tests. These tests are distributed over one with a maximum load at 100 kN, two at 90 kN, two at 80 kN and one static test which failed at 170 kN. The variation in results from similar tests are relatively small compared to many studies on fatigue of composites. They deviate from the average lifetime with approximately 9-15%. This could be due to a benefit from spreading the risk over ten holes at each sample end. Without further discussion, the small amount of tests does probably not show representative results of the actual scatter one would get with 12 or 24 tests. Therefore, the results give an indication of what the lifetime will be at different loadings and will serve as a proper guidance for future tests.

The three proposed curve fits were evaluated based on an adjusted R-square value fitted to data points from five tests. The semi-logarithmic curve fit resulted in the best fit, with the power law fit and the log-log fit in second and third, respectively. If it is desired to predict the lifetime at other fatigue loadings the curve fits are only valid for fatigue loadings with a R-ratio of 0.1 and a tensile maximum load. Whether on is evaluating for loads higher than 100 kN or lower than 80 kN, the semi-log curve fit results in the most conservative prediction. For loads higher than 100 kN, the power law fit will result in the most radical prediction. The log-log curve fit will result in the most radical prediction for scenarios with a maximum load lower than 80 kN. Whether the curve fit will return the most radical or conservative prediction compared to another curve

fit does not indicate which on is the most accurate one. Except from at low-cycle fatigue, where the log-log curve fit appears to be the most accurate based on a static tensile test.

SHM: Optical fibers

The optical fibers may be used in two different ways. The method proposed by Fosså (2014), which considers the strain after n cycles in the area between the top row and bottom row of the holes. This method gives an indication of the load distribution, as well as the magnitude of the strain. It should therefore also be possible to evaluate whether specific bolts is carrying load or not. This might indicate that either the tube has failed in the respective area, or there is a substantial misalignment. Based on thorough testing or proper finite element analysis the relationship between longitudinal strain and hoop strain in one specific point may be established. By knowing the respective relationship, it will be possible to estimate the longitudinal strain in a given position. Based on the comparison between the longitudinal strain measurements and the hoop measurements, it was seen that the behavior of the tube and load distribution could be found through both. It is assumed that it is more practical to use fibers in hoop, both due to the smaller chance of failed fibers, the lower amount of data which is necessary to acquire, the shorter time it takes to apply, and the ease of applying to a filament winding process. Hence, the results are promising regarding the proposed method for SHM.

Another method is to place the optical fibers in a way that they will break if the hole fails. Hence, the optical fibers may either be utilized to study the strain fields or simply to evaluate the distance light is emitted. It was attempted to test this method, but when placing optical fiber on the tube, between the surface of the tube and the metal end fitting the optical fibers failed. This could be tested if a method for embedding optical fibers inside the tube is developed. For the system which have been tested in this study it seems to be of high importance to understand the load distribution. Placing optical fibers in hoop is therefore considered a valuable method for structural health monitoring.

Lifetime prediction

The crushing rate of the tube can be established, but it appears that it varies more than first expected.

The displacement which occurs during the initiation process might be an indicator of how well the bolt holes are aligned. If this is true, then the longer the system is displaced before the crushing rate stabilizes, then the earlier one hole will fail. This might mean that the cycles before failure is very dependent on the quality of the machining of the holes. Additionally, it will probably affect the crushing rate during the propagation phase (phase 2).

Two models for lifetime prediction were proposed, the residual stiffness based model and the basic crushing rate. The residual stiffness model combines data from static tests with data from dynamic tests, and assumes similar displacement at similar load intervals. This assumption is poor because the time dependent effect, creep, is not considered. During the static test, one cycle between 9 kN and 90 kN takes approximately 500 - 600 seconds, whereas during cyclic testing one cycle takes a quarter second. This results in a larger displacement for the static test even though both tests have the same load interval. This effect will result in making the fatigue modulus model less accurate, but more conservative. On the other hand, the model which is based on stiffness tests will only be conducted at given intervals and much less sampling is needed. The crushing rate model must acquire data throughout the entire lifetime. On the other hand it shows the exact behavior of the sample when subjected to fatigue. With data from enough tests, the basic crushing rate model will probably be most accurate.

Lifetime prediction vs. structural health monitoring

There are two ways to consider evaluating the lifetime of the structure. First of all, it is desired to design the structure so that it can sustain a predicted set of loadings for a certain time. Secondly, it is desired to ensure safety by having the ability to monitor the structural integrity at any time during operation. As the time of the Internet of Things is emerging, so is the technology, ease and knowledge regarding real-time monitoring. It is important to make qualified choices when designing a system, hence it important to have the foundation from thorough testing. Additionally, as this design is new, a system for structural health monitoring will enable both increased

safety and increased knowledge regarding the systems response from loads due to operations and the environment.

The systems effect on failure mechanisms

Several failure mechanisms have been observed both on micro and macro scale. Delamination occurs relatively early on in the process. This combined with matrix cracks is probably contributing to the observed behavior during the initiation phase (phase 1). In the propagation phase, crushing occurs by causing fiber kinking, splitting and fiber fracture. The out-of-plane loads, combined with the accumulation of crushed composites / loose material cause parts of the tube to interact with the metal end fitting. This is observed on samples which have been removed before failure. The interaction may affect the lifetime in several ways. Due to friction, there will be a build up off heat which can result in heat degradation of the composite. On the other hand, loose material will become constrained and may help to decrease the crushing rate, as it create a separation between uncrushed laminate and the bolts. In order to evaluate the ideal clearance between the tube and the metal end fitting, the effect of heat-build-up from friction should be evaluated against the temperatures under actual operation.

All samples failed ultimately due to shear out. When the sample was retrieved after failure, it was found that parts of the outer and inner hoop layer was separated from the sample. It can be seen that for a certain distance the hoop layer has been intact as fiber fracture instead of separation has occurred although this distance varies with every hole. Hence, it appears that the cohesive shear strength which between the outermost and second outermost laminae at some point becomes lower than the load which is necessary to cause fiber fracture in the hoop fibers. Which means that at the point the outer and inner hoop layer is released, the contribution to the laminate strength from hoop layers is decreased by 50%. The separation does not occur to the two hoop laminae which is placed in between two other layers. Hence, by adding a 0 ply as the outer and inner lamina, it is expected that the overall lifetime may be increased substantially.

Parameters which affect the cross head displacement

The results from the LVDT showed that the displacement which occurs in the tube could be less than 60% of the value measured as the cross head displacement in the tensile testing machine. The actual displacement of the tube can be divided into displacement due to strain in the tube while the remaining displacement is due to crushing of the laminate. It was found when using LVDTs during testing that the displacement due to crushing and deformation of the hole may vary whether you are considering the upper or lower part and whether you are considering e.g. hole number 5 or hole number 8.

After sample 4B1 was tested the affected area was cut away and a new sample, 4B2, with a shorter length was created. Although the lifetime of the two samples could not be determined, it was apparent that the individual system stiffness varied substantially. This learning should be taken into account because the tested tube is only a fraction in length and complexity of the actual designed tube.

Compared to real life

It would be a far bigger study to compare the given system and fatigue strength to actual loads in industrial applications. But in order to relate the loads and geometries to real-life situations some simple calculations have been performed in order to estimate the dimensions of which the system may be used for in industry.

Offshore oil and gas production   Tubing used for offshore oil and gas are commonly delivered in lengths of approximately 12 meters. It is therefore expected that for every 12 meters of tube there will be a metal connector. Although the dimensions of the sample may not correlate with the dimensions of the final product, it is assumed that there is a linear relationship between the geometrical dimensions and the strength. For this sample 12 meters of tube weights approximately 34 kg. Each metal end fitting may weigh approximately 12 kg. If we assume a maximum estimated load of 150 kN then the system should be able to carry a weight which allow for 3800 meters of tubing. Buoyancy effects, safety factors, weight of fluids, loads due to internal and external pressure and vibrations induced from operation and/or vortexes under the surface have

been neglected. Also any other part of the final product such as an inner or outer liner is neglected. A composite tube, such as the one used in the Thermoplastic Composite Pipe (TCP) created by Airborne Oil and Gas is a good example of a potential final product. With regards to the loads, Skallerud et al (1990) tested flexible pipes within their linear-elastic area of loads up to 250 kN.

Wind turbine   The expected lifetime of a wind turbine operating about 66% of the time is 20 years with an rpm of approximately 10 (Moslemian, 2016). This results in an expected lifetime of up to 10^8 cycles. With the given curve fit the system can sustain 10^8 cycles with a maximum load of approximately 40 kN or 4 tonnes. Currently, the largest wind turbine is the Vestas 164 which produce 8 MW. It has a blade length and weight of 80 meters and 35 tonnes. If we scale it linearly, then the final product based on the sample must have an outer diameter of approximately one meter, which is 4.6 times smaller than the root diameter of the V164 blade. It is still important to mention that the axial loads due to bending at all other angles than 90 and 270 as well as wind loading has not been considered.

It can be concluded that the dimensions of the sample tested may either be scaled up or used for smaller turbines or shallow waters.

Design factors

Uneven loading   As a part of the preliminary studies (Horn, 2015) the distribution of load in the tube was examined. Three strain gauges were placed equally far apart at the hoop center line of the tube.

Ideally the three strains should be somewhat similar, which would have indicated an even load distribution. Instead there were three different slopes. In position 1 the tube was in tension at all times which is expected, as the load ranges between two tensile loads. The slope for the area in position 2 shows a different situation. At first, no load is transferred to the respective area, then as the global loading increases, load / strain also begins to increase. Finally, in position three it is first compressed, before it gradually transfers into tension. A hypothesis regarding these results is that there is an unevenness somewhere in the system. It is assumed that it was

due to the failed bolts in the tensile test machine, but it may also have been due to the position of the bolt holes in the tube. Hence, in order to avoid uneven loading, it is important to both focus on the machining of the sample as well as the assembly of the system.

e/d - ratio   The specimen is assumed to ultimately fail when the crushed distance causes the e/d-ratio to reach a critical point. Hence, by simply increasing the length of the metal end fitting which enables one to increase the e/d-ratio, the lifetime can be increased. On the other hand, one of the main reasons to use composite tubes is the benefit of a weight reduction. If the size of the metal end fitting is increased, the weight will also be increased, which introduces another field of optimisation. A simple estimate can be created by using values from Chapter 5.3.3 and assuming a maximum load of 90kN. Increasing the distance from the edge of the hole to the edge of the specimen with 10 mm will increase the lifetime with 115000 cycles. This is a simple estimate, but it shows how big effect the e/d-ratio may have on the lifetime.

Leakage-before-failure   The results from the dynamic testing have been divided into three phases. By examining the displacement between phase 2 and 3 in the weakest sample, a threshold for leakage-before-failure may be found. This threshold may be used further in design of the metal end fitting, when evaluating the optimal position of sealing systems.

Failed test setup

As mentioned, the jumps that occurred during some of the tests have been assumed to be due to failed bolts in the tensile test setup. Because the bolts failed one at a time the samples have probably been subjected to different uneven loadings. The uneven loading makes it difficult to replicate the tests both experimentally and numerically. On the other hand, the results may prove to be useful when trying to understand the systems behavior when subjected to both axial loading and bending. Therefore, the analysis of the results has been conducted according to the plan.

Because there is a varying quality of the tested samples, the sample size should be relatively high. By considering sample 4C and 4D it is apparent that there is a significant scatter in between similar tests. By only testing one or two samples for each system and load, the confidence

level will be remarkably low. It was decided to rather test few samples at several different loads in order to gain a basic understanding of the systems response to different load scenarios. Nevertheless, at two different loads, two samples were tested. The maximum variance in lifetime was 15% of the mean lifetime. In fatigue studies, it is not uncommon that the results can vary with 5% - 60% ((Perreux and Joseph, 1997) and (Kaynak and Mat, 2001)). Either way, in future studies it should be considered to increase the sample size in order to increase the quality of the study.

Another problem which is introduced by the unbalanced loading of the tube is the accuracy of the measurements. The measurements retrieved will either give a mean displacement / loading or a local displacement / loading. It is therefore complicated to know whether the values measured with the applied sensors are the largest, lowest or anything in between. The only way this seems applicable is through the use of distributed fiber optic sensing.

An important learning from this scenario which caused uneven loading to the samples is the importance of high quality in production. Ideally the holes which are machined in the specimen should line up concentrically with the holes in the metal end fitting. If there is one or more of the holes does not line up, events similar to the uneven loading which was experienced may occur. It should therefore be taken specific care when cutting and milling the samples.

Standardization

The test program has been structured based on the amount of time at hand and previous studies. It has not been based on any standards, hence the results may not be entirely transferable to further studies or for comparison with other studies. On the other hand, because this study is based on the practice of many other studies, it appears that most of the procedures are very similar to those described in standards such as ASTM D3479/D3479M - 12. Additionally, according to the same standard. The amount of tests that have been run barely certifies this study as preliminary and exploratory.

A highly detailed procedure has been written in the Appendices. The level of detail should be enough to ensure proper replications of the production and testing of the samples.

Chapter 7

Conclusion

The purpose of the thesis has been to evaluate the fatigue properties of a given system. The system consists of a GFRE tube, two metal end fittings and 20 bolts and bushings. The most important target was to establish a S-N curve and evaluate methods to use optical backscatter reflectometry for structural health monitoring. Secondly, it has been of interest to analyze the fatigue behavior throughout the entire lifetime.

Several variations of S-N curves have been established, whereas the S-N curve for ultimate failure is of highest importance. The curves are based on data from five tests, one test at 67% of critical load, two at 60% and two at 53%. The main S-N curve has been successfully curve fitted with three different curves based on a power law equation, a semi-logarithmic equation and a log-log equation. Several models which were meant to better understand the life cycle during fatigue was explored. It was established that the stiffness of the sample remains relatively constant over the life time. It was also established that the displacement/crushing behavior is inverse of the sigmoid logistic function.

Using optical fibers for structural health monitoring have shown positive results. It was proven that it is important to monitor how the load is distributed over the ten bolts at each end of the tube. Measure strain at different loads and times enables the opportunity to evaluate how the load distribution varies. Placing the fibres in hoop does return valuable results regarding the load distribution. Another proposed method to measure the magnitude of the crushed distance is to install sacrificial fibers which are meant to break when a predefined limit is reached.

Chapter 8

Recommendations and further research

This study shows how the lifetime of a given system can be estimated based on different known load scenarios.

If it is desire to improve the current knowledge regarding the given design, the following work is advised.

- The ease of commissioning and decommissioning for the tests have a high potential for improvements. A first step should be to acquire bushings with a length which will fit inside the slot on the metal end fitting.

- Run one or several high cycle dynamic tests in order gain a better understanding of the fatigue properties when tested at lower loads.

- Cumulative damage, with regards to different loading scenarios throughout the lifetime has not been considered in this study. The study of such damage will increase the understanding of how the system will respond to loads from actual operation.

- Future studies should follow applicable standards.

- The distance a specimen has been displacement when ultimate failure occurs should be evaluated against finite element analysis.

In order to create a more complete design guide for similar systems the following work should be performed:

- Similar studies should be run with focus on study the effects of:

  - Scaling the system and looking at the differences for a given loading

  - Varying the bolt size and test for a given loading

  - Varying the r-ratio

- The strength contribution from hoop plies should be evaluated in order to optimize the layup.

- The heat generation from interaction between the composite tube and the metal end fitting should be evaluated.

In order to improve the NDT solution for detecting failure the following work should be performed:

- Use FEA to evaluate the relationship between the hoop strain and longitudinal strain in critical locations.

- Develop and test a method for embedding optical fibers in the composite tubes.

Bibliography

Bhandari, V. B. (2001). *Introduction to Machine Design*. Tata McGraw-Hill Education.

Cox, K. B., Vedvik, N.-P., and Echtermeyer, A. T. (2014). Flexural Fatigue of Unbalanced Glass-Carbon Hybrid Composites. *Journal of Solar Energy Engineering*, 136(4):041011.

DNV-GL (2013). *DNV-OS-C501 Composite Components*. DNV-GL.

Dons, K. (2013). Filament Winding of Composite Tubes. Master's thesis, NTNU.

Fosså, A. (2014). Bolted Metal End-Fittings for Composite Tubes. Master's thesis, NTNU.

Grave, J. L., Håheim, M. L., and Echtermeyer, A. T. (2015). Measuring changing strain fields in composites with distributed fiber-optic sensing using the optical backscatter reflectometer. *Composites Part B: Engineering*, 74:138 – 146.

Horn, M. (2015). Fatigue testing and modelling of composite tubes. Master's thesis, Norwegian University of Science and Technology.

Joseph, E. and Perreux, D. (1994). Fatigue behaviour of glass-fibre/epoxy-matrix filament-wound pipes tension loading tests and results. *Composites Science and Technology*, 52(4):469 – 480.

Kah, P., Suoranta, R., Martikainen, J., and Magnus, C. (2014). Techniques for joining dissimilar materials: Metals and polymers. *Reviews on Advanced Materials Science*, 36:152–164.

Kaynak, C. and Mat, O. (2001). Uniaxial fatigue behavior of filament-wound glass-fiber / epoxy composite tubes. *Composites Science and Technology*, 61:1833–1840.

Lee, C. S. and Hwang, W. (2000). Fatigue life prediction of matrix dominated polymer composite materials. *Polymer Composites*, 21(5):798–805.

Manyika, J., Chui, M., Bisson, P., Woetzel, J., Dobbs, R., Bughin, J., and Aharon, D. (2015). *The internet of things: mapping the value beyond the hype.* McKinsey Global Institute.

Moslemian, R. (2016). Composites in offshore/marine structures. Lecture for TMM4260:Offshore Materials, NTNU.

Pederson, J. (2008). Finite element analysis of carbon fiber composite ripping using abaqus. Master's thesis, Clemson University.

Perillo, G. (2014). *Numerical and Experimental Investigation of Impact Behaviour of GFRP Composites.* PhD thesis, NTNU.

Perreux, D. and Joseph, E. (1997). The effect of frequency on the fatigue performance of filament-wound pipes under biaxial loading: experimental results and damage model. *Composites Science and Technology*, 57:353–364.

Persson, E., Eriksson, I., and Zackrisson, L. (1997). Effects of hole machining defects on strength and fatigue life of composite laminates.

Samborsky, D. D., Wilson, T. J., and Mandell, J. F. (2009). Comparison of tensile fatigue resistance and constant life diagrams for several potential wind turbine blade laminates. *Journal of Solar Energy Engineering January 6, 2009 131(1):01100.*

Saunders, D., Galea, S., and Deirmendjian, G. (1993). The development of fatigue damage around fastener holes in thick graphite/epoxy composite laminates.

Skaar, M. W. (2015). Modeling and testing of impact damage in composite pressure vessels. Master's thesis, NTNU Trondheim.

Strathman, J., Watkins, S. E., Kaur, A., and Macke, D. C. (2016). Strain monitoring of a composite wing. *Proc. SPIE*, 9803:980346–980349.

Talreja, R. and Singh, C. V. (2012). *Damage and Failure of Composite Materials.* Cambridge Universal Press.

Thoppul, S. D., Finegan, J., and Gibson, R. F. (2009). Mechanics of mechanically fastened joints in polymer–matrix composite structures–a review. *Composites Science and Technology,* 69(3):301–329.

Appendix A - Acronyms

CR Crushing rate

D Displacement

E Stiffness / Elastic modulus

F Load

FW Filament winding

GFRE Glass fiber reinforced epoxy

IoT The internet of things

LVDT Linear variable differential transformer

L Length

$m_{f/e}$ Mass of fiber or mass of epoxy

NDT Non destructive testing

OBR Optical backscatter reflectometer

$p_{f/e}$ Density of fiber or density of epoxy

SG Strain gauge

SHM Structural health monitoring

V_f Fiber volume fraction

Appendix B - Machines, tools and materials

Table 1: Equipment and software used for tensile testing

Type of equipment	Description
Tensile testing machine	500 kN Schenk
Controller	Instron
Software	CatmanEasy, OBR4600, Luna OBR V3.12.2
Interface	Spider 8
Strain measurements	Strain gauges, Optical Backscatter Reflectometer
Displacement and load	Instron

Table 2: Equipment used for filament winding

Equipment	Specification
Filament winding machine	Microsam MAW 20 LS 4/1
Fibre tensioner for FW	METS-8
Filament winding software	CNC Winding Commander 8.0
Winding Expert	Spider 8
Mandrel	Tapered steel mandrel

Table 3: List of materials used in production

Material	Specific name	Purpose
Glass fibre	HyPer-tex TM W2020 R-Glass fibre	
Epoxy resin	Epikote Resin MGS RIMR 135	
Epoxy hardener	Epikure MGS RIMH 134	
Release wax	Renlease QV5110	Decrease friction at the GFRE-steel interface
Sticky tape	-	Fill in hole between end spheres and mandrel
Acetone		Remove epoxy from tools

Table 4: Tube machining tools

Operation	Machine/tool
Cutting tube	Horizontal band saw
Drilling holes	Three axed milling machine with a modified glass/tile drill bit
Reaming holes	Hand drill with 10 mm wolfram carbide reamer

Appendix C - Procedures - Production

Filament Winding

NOTE: All filament winding took place as part of the Project thesis. The following procedure is based on previous experiences.

Read this the first day of planning the filament winding:

- Verify that you have all necessary material, such as epoxy, glass fiber mats, release wax, mandrel and peel ply.

- Book the room on designated calendar

- Create winding program

On the day of production

Protective gear:

- Longsleeves, cheap shoes and a lab coat/suit or similar.

- Gloves when handling epoxy

- Protective glasses, at all times

- Respirator during hand layup, epoxy mixing and work with acetone.

Timespan 6.5 hours in total (2 hours preparation, 3.5 hours operation with wet epoxy, 1 hour cleaning).

1. Preparations

    (a) Glass fiber - Hypertex must be placed in the tensioning cabinet. Before this, every tiny strand of glassfiber on the bobbins and in the cabinet must be removed. Very important in order to avoid ruptured tows and poor quality samples.

    (b) Mat layup - Place a plastic sheet over the entire table in the composite lab. On top, place 4 plastic sheets of 400 x 230 mm. Ensure that you have long rulers, a knife, squegee and gloves at hand. Verify that there is enough 0/45/-45 fiber mats left. Cut out 2 x (the length of the tube that you intend to make). Estimated width of mats:

        • 1 (inner) - 32 cm

        • 2 - 33.3 cm

        • 3 - 33.7 cm

        • 4 (outer) - 34.2 cm

    (c) Clear the path between the composite lab and the plastic lab.

    (d) Mandrel

        • Steel mandrel - Mount in filament winding machine, apply release wax, create new program based on the current mandrel and mount position, fill gaps and openings with sticky tape.

        • Plastic mandrel - Machine tubes based on the the metal end fittings used in the mandrel, mount and make new program.

        • Both - Place tape on the outer rods, in order to make 4 points 90 degrees apart. These points will indicate the position of the weld lines for the four fiber mats that will be applied.

    (e) Program - Speed = Default

    (f) Winding editor by Microsam

        • 6 mm hoop plies and 5 mm helical plies

Table 5: My caption

Step	Width	Angle	Direction	Frames (based on the mandrel file)
1	5	90	Backwards	9-11
2	4	12.7 Optimized Pattern 3/2	-	2-18
3	5	90	Forwards	9-11
4	5	90	Backwards	9-11
5	5	90	Forwards	9-11

- Remember to change the distance to the zeropoint (given in the mandrel file) in "Winding editor -> Winding parameters" before you add winding operations in Winding editor.

(g) Epoxy mix

- Mats: 1.54 kg resin + 0.46 kg hardener

- Winding bath: 0.77 kg resin + 0.23 kg hardener

(h) Responsibilities This is a 2-3 man job. It is therefore recommended to have one person who wears plastic gloves and one person who operates the knife in order to remove excess fibers in the feeding system. This will help minimize the consumption of plastic gloves.

2. Winding - see table 1 for overview

(a) Stick fiber to the mandrel

(b) Turn on the correct fiber tension

(c) Press play

(d) Stop after the first layer, turn of fibertension.

(e) Mat application

- Measure circumference

- Cut out fibermat

- Wet fiber mat with epoxy

- Carry out and apply to the mandrel at the designated weld line

- Notice from table 1 which layer should be the outermost.

TABLE 3.1: Production summary. Letters under section refers to letters in Figure 2.3

Ply nr.	Fiber angles [deg]	Method	Joint placement	Fiber tension	Sections Fig. 2.3
1	[90]	wound	–	15 N	A,B,C,D,E
2-4	[-45/45/0]	mat	0	–	B,C,D,E
5	[±12, 7]	wound	–	15 N	A,B,C,D,E
6-8	[0/45/-45]	mat	180	–	C,D,E
9	[90]	wound	–	35 N	A,B,C,D,E
10-12	[0/45/-45]	mat	90	–	D,E
13	[90]	wound	–	35 N	A,B,C,D,E
14-16	[0/45/-45]	mat	270	–	E
17	[90]	wound	–	35 N	A,B,C,D,E

Figure 1: Overview

- Use your hands, with gloves, and make sure that all air bubbles are removed and that the weld line is flush

(f) Continue similarly for the remaining production process. It may be necessary to rise the epoxy bath two notches up after the third mat.

3. Decommisioning

- Do not forget to clean the composite lab

- Make sure to mix all unmixed resin or hardener, if tossed in the trash without being mixed out it will pose an environmental threat as well as the trash can will smell very intense.

- Clean the big roller thoroughly!

- Remember to continuously rotate your produced tube

4. Curing process: Rotate for 24 hours in room temperature, then place in oven at 80 C for 15 hours.

Figure 2: Photo of setup at milling machine. Including mill, chucks and tube mounted on the delehode.

Comment regarding the tensioning system   Because the cabinet for the tensioning system is not suited for the glass fiber drum, a solution have been created at NTNU to connect the two together. This solution makes it possible to feed fibers from the outside of the cabinet in to the fibre tensioner. In addition, a steel mandrel has been produced for the respective tube. To be able to pull the composite tube of the mandrel, it has been designed with a taper from one end to the other. The mandrel is installed into the filament winder.

Machining

See photo 2

- Remove mandrel in mandrel extractor

- Cut in 200 - 300 mm long specimens

  - Water cooled (in order to prevent heating of tube) in horizontal band saw.

  - The rotating diamond saw will not give a leveled cut when cutting tubes

- Drill holes – 0%-1% tolerance – 9.8 mm

  - Use CNC machine

    * Spindle rate of 1000 rpm

    * Feed rate 10 mm/min

  - Make sure to place holes both at mat weld point and not at mat weld point

  - According to Persson et al. hole machining defects such as delamination may have a negative effect on the structural integrity of the holes. The recommended KTH method is complicated to utilize for hole machining on curved surfaces such as tube s. At a later stage it is recommended to evaluate whether or not the current method of machining holes should be improved.

  - These holes need to be concentric with the respective holes in the end fitting and they need to be press fit with the designated bearings. The currently used method for drilling holes is a three step procedure. First, the tube is placed inside the end fitting and center marks are made. Then the tube is locked into a "rundmatingsbord / delehode" and which is positioned on a mill. Holes can then be drilled 36 degrees apart from each other. The drill bit used was a modified 10 mm drill bit designed for cutting tiles and glass.

- Ream holes

  - Wolfram carbide reamer from Sandvik Coromant, see fig 3

  - Hand held battery drill - Speed 500 rpm ish

- Sand inside of tube with 220 grit

- Degrease hubs with acetone

Figure 3: a) Bosch CYL-9 10 mm b) grinding of drill bit

- Tightened bolts to 114 Nm using a torque key

- After the drilling process, each hole was reamed with a wolfram carbide reamer from Sandvik Coromant. Finally, all the edges were sanded with a 400 grit sandpaper.

Appendix D - Sensors

Basic difference between OBR and Strain Gauge

In this chapter, the main characteristics of strain gauges and optical fibers, as well as the differences between the two will be addressed.

Each strain gauge used in this study covers a small area of approximately 5 mm x 2 mm. It will measure the mean strain over the entire area by measuring the adjusted resistance due to strain. The signal acquired resembles the current through the strain gauge at a set frequency. We have been measuring at 50 Hz. The optical backscatter reflectometer on the other hand sends a light through an optical fiber. Due to difference in surface roughness, the OBR can read off deformations or other anomalies. Analyzing data from the OBR is sort of like analysing data from a high number of strain gauges coupled in series. Due to all the data points gathered at each measurement a normal file may be 65 MB. So, even if it was possible, it would not be very effective to conduct OBR measurements 50 times every second. Through the strain gauge configuration it is therefore possible to acquire data continuously for a rather limited length. In an opposite way, OBR measurements can measure strains in over large distances (up to 70 meters), but only at a time instance. Because measuring strain through strain gauges is the industry standard and OBR is a relatively new technology it is considered best practice to use strain gauges as a reference to the OBR.

Linear variable differential transformer

A LVDT is a sensor which is used to measure a displacement between two objects. Mechanical movement is transformed to an electrical signal. One of the main benefits is the low friction

which means that hysteresis should be negligible. On the other side, it is not frictionless, and can therefore not be subjected to high frequency fatigue as it tends to cause an increase in friction over time. The increase in friction is possibly due to wear or heat degradation of the lubrication.

Appendix E - Procedures - Testing

Burn off tests

Use ceramic cups. Take the weight off the cups, then the weight of the cups with the sample. Then put the samples in the oven, heat it to 550 C and leave it for 5 hours, see figure 4. Let it cool down, then take the weight of the cups with the fibers.

Static tensile test

Procedure for testing the tensile strength and stiffness of the sample.

1. Fasten the machined sample with installed sensors in the metal end fittings.

   - Bearings: It may be difficult to get all the bearings in place. The maybe worst, but most effective practice is to ream the holes in the composite tubes through the holes in the metal end fitting. Then use a Ø10 mm rod and a rubber hammer the knock the bearing in place.

   - Bolts: In this study the bolts were tightened using a torque wrench. No washers were used.
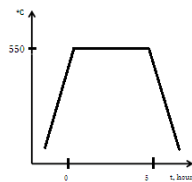
Figure 4: Heating cycle for burn off test

2. Fasten the entire sample with metal end fittings in the lower part of the tensile test machine.

3. Connect sensors.

4. Prepare Catman, with the correct sensors, sampling rate, data storage (ASCII+Channel info) etc.

5. Evaluate whether all sensors work properly, reset SG and make a reference file for the optical fibers.

6. Turn on the hydraulic system.

7. Position the jig properly with the console. If only tensile test, then position the jig in -9ish mm.

8. Connect the upper part of the tensile test machine.

9. Prepare the console. Set the proper limits and event detection. The displacement in this study was run as Position -> Ramp -> 0.01 mm/sec. When setting the displacement distance, the direction also must be decided. When applying tension it should be positive and when downloading it should be negative.

10. Press play.

Dynamic tensile test

1. The preparation is similar to steps 1. -9. in the procedure for running the static tensile test.

2. Instron console settings:

   - Event detection - number of cycles: Load - > Event detection -> #5 -> Set number of cycles and "Hold".

   - Limits: Similar to static testing.

- Mean load: You must displace the sample until the desired mean load has been reached. Then press Load -> Go to -> Mean load, in order to keep it at mean load despite creep effects.

- Amplitude and frequency: Load -> Waveform -> Cyclic/sine, 4 Hz, amp load.

- Amplitude control: Turn on in order to ensure that the desired maximum and minimum loads are reached.

- Press play.

Example of how the dynamic tensile test with stiffness measurements were conducted.

1. Static tensile loading

   - Load sample at 0.01 mm/sec up to 70 kN.

   - Unload at 0.01 mm/sec down to 0 kN.

2. Dynamic tensile loading 1000 cycles.

3.

4. Load sample at 0.01 mm/sec to 38.5 kN.

5. Run fatigue test at 1000 cycles.

6. Unload at 0.01 mm/sec down to 0 kN.

7. Static tensile loading - Download to 0 kN, then run the same procedure.

8. Repeat, repeat, repeat for desired intervals.

Microscopy

At the machine shop: Samples were cut out using the vertical bandsaw.

At the composite lab: Samples were placed in a cup of uncured epoxy and then left for curing.

Figure 5: Sanding machines at Metallurgy lab at IPM.

At the metallurgy lab: Samples were sanded and polished, figure 5 shows the equipment which was used. The sanding process was performed with the following grits: 80, 120, 240, 400, 800, 1200, 4000.

The samples were evaluated using a Zeiss microscopy, see figure 6. The magnifications used were: 50x, 100x and 200x.

Figure 6: Microscope at Metallurgy lab at IPM.

Appendix F - Overview of tests

Test 4A

Purpose

Run static test in order to benchmark the strength of sample 4.

Key test parameters

Geometrical data

- Total length: 200 mm

Sensor placement

Optical fibers   Three sets of optical fibers were mounted on the sample.

Strain gauges   Six strain gauges were used. Three around the hole, and three placed longitudinally in the middle of the tube at different places on the circumference.

Loading

- Displacement rate = 0.01 mm/sec.

Comments during test

- Performed OBR measurements at the following displacements: 1, 1.5, 2, 2.5, 3, 3.5, 4, 4.5 mm and maximum displacement

Test 4B1

Purpose

Run dynamic test at high mean load with R-ratio=0.1.

Key test parameters

Geometrical data

- Total length: 208 mm

Sensor placement

Optical fibers

Strain gauges   Three strain gauges were placed at the middle of the tube.

Loading

- R-ratio = 0.1

- Max load = 70 kN

- Min Load = 7 kN

- Mean load = 31.5 kN

- Amp load = 38.5 kN

Comments before test

-

Comments during test

-

-

-

- Failed ultimately in the weld on the bottom end fitting.

Test 4B2

Purpose

Run dynamic test at high mean load with R-ratio=0.1. Evaluate if it is possible to use middle part of previously tested samples.

Key test parameters

- Ran at 38.5+-31.5 kN @ 4 Hz for 112804 cycles until metal end fitting failed

- Clear signs of delamination, crushing and disappeared debris

- Rate of displacement per cycle increases with time

- Fatigue modulus – appears to have a linear relationship within certain intervals of the lifetime. As opposed to have a linear relationship the entire lifetime.

- Elastic modulus – stiffness increases remarkably between the 1st and 2nd /3rd, but is just slightly increasing every cycle. Elastic modulus also appears to be higher for the shorter tube. Item Displacement at max load after n cycles - Linear logarithmic relationship

- 5001 cycles irregularity Probably caused by the rotation of the system.

Geometrical data

- Total length: mm

- Length between holes 120? mm

Sensor placement

Optical fibers

Strain gauges Three strain gauges were placed at the middle of the tube, similar to sample 4B1.

Loading

- R-ratio = 0.1

- Max load = 70 kN

- Min Load = 7 kN

- Mean load = 31.5 kN

- Amp load = 38.5 kN

- Frequency = 4 Hz

Comments before test

- Evaluating stiffness @ 1, 2, 1000, 2000, 3000, 4000, 5000, 15000, 25000, 35000

Comments during test

- It should be evaluated how the loading unloading should be performed, e.g. unload down to start / 0 mm, or unload to x mm where the load Is zero / unload until loading is zero.

- Strain gauges: After approximately 15000 cycles, Mid3 is subjected to compression when the structure is unloaded. Between 10-20 kN it is tensioned again. Possible causes: Poor adhesion to the tube has caused irregularities?

- Plot displacement vs time in order to get a visual of the crushing behaviour. Potentially look at the slope of the curve at after different amounts of cycles.

- Logged at 10 Hz, seemed fair

- Because displacement is increasing and before 4000 cycles we went back to zero, there was some more time for relaxation of the composite

- Static4001: Started at 0 mm, ended at 2.5 mm

- After dynamic 5000: rotated clockwise (seen from above) 180 degrees

- After static 5001: rotated back

- What parts of the displacement during fatigue are we seeing? Is it creep due to a mean loading at 38.5 kN? Is it crushing due to cyclic compression at the top of the hole? Is it some sort of shear out on the sides of the hole?

- Is the tube actually being subjected to the maximum and minimum load during fatigue cycling?

- After 1000 cycles: about 21 in end fitting, bolt and tube

- After 1500 cycles: about 35 in bolt, 30 in end fitting and 30 in the tube

- Measured (probably incorrectly) with an infrared thermometer from Biltema, article 17-236

Test 4C

Purpose

Run dynamic test at high mean load with R-ratio=0.1. With maximum load = 70 kN. Also use LVDT sensor to evaluate the actual displacement of the tube.

Key test parameters

Geometrical data

- Total length: 200 mm

Sensor placement

LVDT LVDT (RMPe) placed as close to one of the upper holes as possible

Strain gauges Strain gauge in the middle below the LVDT.

Optical fibers Optical fibers near the same hole.

Loading

- R-ratio = 0.1

- Max load = 90 kN

- Min Load = 9 kN

- Mean load = 49.5 kN

- Amp load = 40.5 kN

- Frequency = 4 Hz

Comments before test

- Run static test at: 1,2,3,4,5,100,500,1000,10000,20000,(30000)

- Run OBR scan at Mean load for 1,2,3,4,5,100,500,1000 -> every thousand

Comments during test

- During dynamic 99: forgot to remove LVDT

- After Static 1: moved lock ring for LVDT from quarter bottom to middle.

- The $Dynamic_{9999}$ logging was not started before 5650 cycles was reached.

- After approximately 12500 cycles a loud noise was heard. It resulted in an immediate displacement of approximately 0.5 mm. The rate of displacement per cycle also increased after the bangdiggety.

- After 15260 cycles it was approximately 0.2 mm ish

- It finally ruptured on the bottom half after 23823 + not counted cycles, which is approximately 100+1+1+1+1+1+1==23930

- 200 cycles before failure, the clearing over the bottom holes was approximately 2 mm

Test 4D

Purpose

Run dynamic test at high mean load with R-ratio=0.1. Gain better understanding of phase 1 fatigue properties.

Key test parameters

Geometrical data

- Total length: 208 mm

- Length between holes 153 mm

Sensor placement

Optical fibers Optical fibers were placed longitudinally between hole 1 and 10. They were also placed in hoop under the hole rows. The postitions of different geometrical points is shown below. End of plastic tube: 10,209 m ish Weird peak: 10,58488 MidSG10 = 10,3159 Found with 0,8 and 0,8 on OBR SG options Hoop: 33 mm from bottom, 5 mm from hole edge

Strain gauges Four strain gauges were used, all pointing longitudinally. In the area 10, one strain gauge was placed below each hole and one strain gauge was placed in the middle. One strain gauge was also placed in the middle of area 5.

LVDT Two LVDTs were used. Because of the dimensions of the LVDTs, one measured the entire displacement of the time, whilst the other measured the displacement of the lower half of the tube. They were placed between area 1 and 10. The large LVDT was fastened using a jig created from bent aluminum plates, a lock ring and six washers. The small LVDT was fastened using a lock ring.

Loading

- R-ratio = 0.1

- Max load = 90 kN

- Min Load = 9 kN

- Mean load = 49.5 kN

- Amp load = 40.5 kN

Comments before test

- Run static test at: 1,2,3,4,5,100,500,1000,10000,20000,(30000)

- Run OBR scan at Mean load for 1,2,3,4,5,100,500,1000 -> every thousand

Comments during test

- Startup issues: Weird start, probably because I attempted to fasten the upper bolt by moving the entire top jig of the tensile testing machine up.

- Cycle 4 -5: Somehow at the max load at cycle 4, the max load limit of 92 kN was reached. The console was set to unload the sample in such an event. Therefore as I was in the process of setting the load to 90 kN, the load dropped to zero, and when I hit the set button it bumped back up to 90 kN.

- Cycle 7-99: Sample rate was 25 Hz, instead of 50 Hz. I forgot to remove the LVDTs.

- Cycle 1000: Got disturbed, ran the test to 95 kN.

- At approximately 1500 cycles, the strain began to increase in all strain gauges. Halfway through the process, the strain at mid 5 dipped back, whilst the strain strain in mid 1 and bottom 1 continued to increase. The strain in top 1 remained static.

- At approximately 6500 cycles there was a drop in strain at mid 1 and top 1, but increase in bottom 1. Also a slight increase in mid 5.

- Static cycles: 1,2,3,4/5,6,100,500, 1000, 10000, 20000

- Dynamic cycles: 7-99, 101-499, 501-999, 1001-9999, 10001-19999

- OBR measurements: 1,2,3,5,6,100, 500, 1000, 10000 @90 kN

- While uploading to 10000 small sounds were heard every 5-10 seconds. No signs were observed in the graphs in the visualisation module. Same noises were heard while unloading, it was undoubtedly from the top end fitting. While uploading to 20000, no noises were heard.

- 12500 cycles: Loud noise was heard. A drop was seen in the strain gauges in the area of hole number 1, whilst a rise was seen in the mid 5 strain gauge. This indicates that either hole number 1 and/or some of the holes next to it have failed.

- At approximately 15000 cycles, the top of bottom hole 10 reached the edge of the end fitting at maximum loading.

- The sample failed completely by shear out at 32658 cycles.

- It was displaced/crushed 3.08 mm before it began to displace drastically.

Test 4E

Purpose

Run dynamic test at high mean load with R-ratio=0.1.

Key test parameters

Geometrical data

- Total length: 208 mm

- Length between holes 153 mm

Sensor placement

Optical fibers   Optical fibers were placed longitudinally between hole 1 and 10. They were also placed in hoop under the hole rows. The positions of different geometrical points is shown below.

Strain gauges

LVDT

Loading

- R-ratio = 0.1

- Max load = 80 kN

- Min Load = 8 kN

- Mean load = 44 kN

- Amp load = 36 kN

Comments before test

- Run static test at: 1,2,3,4,5,100,500,1000,10000,20000,(30000)

- Run OBR scan at Mean load for 1,2,3,4,5,100,500,1000 -> every thousand

Comments during test

-

-

-

-

Test 5A

Purpose

Run dynamic test at high mean load with R-ratio=0.1. 80 kN max load. Also evaluate the difference in hoop strain in area beneath holes and area in the middle beneath two holes.

Key test parameters

Geometrical data

- Total length: 202 mm

- Length between holes: 147 mm

- Distance from top of hole to end: Bottom=17.5 ; Top= 17.8 mm

Sensor placement

Optical fibers   Optical fibers were placed longitudinally between hole 9 and 10, and between hole 10 top and bottom. They were also placed in hoop 6mm under the hole rows on top and bottom. Additionally on the bottom, it was measured 10 mm below the hole rows.

Strain gauges   Two strain gauges were placed in hoop, below the bottom row. They were placed at an interval between 8-11 mm ish away from the hole. The first strain gauge was placed below hole 7. The second strain gauge was placed between hole 7 and 8.

Loading

- R-ratio = 0.1

- Max load = 80 kN

- Min Load = 8 kN

- Mean load = 44 kN

- Amp load = 36 kN

Comments before test

- Run static test at: 1,2,3,1000,10000,20000,50000, 80000, 120000

- Run OBR scan at Mean load for 1,2,3,1000,10000,20000,50000, 80000

- It appeared that the OBR fiber has broken during installation. It seems as if only the first 20 centimeters will be valid.

Comments during test

- Ran at 0.1 mm/sec during uploading, switched to 0.01 mm/sec for the downloading and remaining static tests.

- Performed OBR measurements at 80 kN at cycle 1, 2,3,1000,10000,20000,50000, 52091,80000

- Extremely loud and unpleasant noise was heard when the when the system was held after the first 999 cycles. Børge said it was nothing to worry about.

- At approximately 4000 cycles a loud noise combined with a rapid change in displacement occured.

- After 52090 cycles, the upper metal end fitting failed in the weld. Composites 3 - Steel 0

- Continued the test after one week (11th of May). The Metal end fitting was welded together by Carl-Magnus. Before the metal end fitting was put back in place, the holes had to be sanded. The entire process of removing and replacing the MEF has probably had some impact on the results, which must be taken into account.

- 25700+52090 noise +jump

- At 100065 cycles, the sample failed completely. small crushing noises were heard just seconds before failure.k

Test 5B

Purpose

Run dynamic test at high mean load with R-ratio=0.1.

Key test parameters

Geometrical data

- Total length: 208 mm

- Length between holes 153 mm

Sensor placement

Optical fibers   Optical fibers were placed longitudinally in positions 10-10 and 9-10. They were also placed in hoop under the hole rows and above the bottom row.

Strain gauges   SG were placed on the center line of the tube, longitudinally. It was placed to the left of the 10-10 fiber. Another SG was placed below the fiber in hoop at hole 8.

In addition, 4 strain gauges were placed at the four faces of the upper metall end fitting.

Loading

- R-ratio = 0.1

- Max load = 80 kN

- Min Load = 8 kN

- Mean load = 44 kN

- Amp load = 36 kN

Comments before test

- Run static test at: 1,2,3,4,5,100,500,1000,10000,20000,(50000)

- Run OBR scan at Mean load for 1,2,3,4,5,100,500,1000 -> every thousand

Comments during test

- Commenced test at 0800

- Static tests and OBR measurements were performed at cycle: 1, 2, 3, 100, 1000, 10000

- At the end of the 999 cycles, a loud noise occurred as the system was held. This is similar to the occurrence after 100 cycles for 5A1. This time the noise lasted for at least five seconds, until I finished the program and turned of the hydraulics. Then I turned the hydraulics back on immediately.

- It is observed that the jig is not loaded correctly. One side of the upper metal end fitting is taking the entire load.

- After 24400 cycles, a loud noise occurred together with a jump in the displacement. This is similar to what has occurred on every test before. This time it could be compared to the SGs at the metal end fitting. After the jump, the uneven strain distribution on the front and back face was much more balanced, though still slightly unbalanced. This correlation shows either that one side, and one hole is loaded much more because of a cricket metal end fitting, or that the metal end fitting ended up cricket because of a cricket tube or a cricket alignment of the holes.

- With time (and cycles) the system becomes increasingly unbalanced, still much less than originally.

- At 40000 cycles, another noise and jump occurred. This one was smaller than the first one. For approximately 1000 cycles, the displacement was remarkably larger than normally. Odd. Why?

- At 92000 cycles a third noise and jump occurred. This time, the load distribution seems to have flipped. Now the front panel on the MEF is barely loaded, while the load in the back panel is subjected to and increased load. The unevenness was increasingly balanced with time, but still the back panel suffered a three times as high load. Before the flip, the front panel suffered only 1.4 times as high load as the back panel.

- At 114000 cycles a new smaller jump and noise occurred. After this jump, the load distribution seemed to be more or less unchanged. But the crushing rate increased substantially.

- At 116000 cycles the slope increased much more.

- Ultimate failure occurred at 119714 cycles.

Test 5C1

Purpose

Run dynamic test at high mean load with R-ratio=0.1.

Key test parameters

Geometrical data

- Total length: 208 mm

- Length between holes 153 mm

Sensor placement

Optical fibers   Optical fibers were placed:

- Hoop: Bottom, between 10, 9, 8, 7, 6, 5, 4, 3, 2 (6mm away from the hole)

- Longitudinally in positions 10-10,9-9, 8-8, 7-7. 6-6, 5-5, 4-4, 3-3.

- Hoop: Top, between 2, 1, 10, 9, 8, 7 ,6, 5, 4 (6mm away from the hole)

Strain gauges   SG were placed on the center line of the tube, longitudinally. It was placed to the right of the 6-6 fiber. In addition, 4 strain gauges were placed at the four faces of the upper metall end fitting.

Loading

- R-ratio = 0.1

- Max load = 100 kN

- Min Load = 10 kN

- Mean load = 55 kN

- Amp load = 45 kN

Comments before test

- Run static test at: 1,2,3,100,1000,5000,10000. (20000)

- Run OBR scan at max load at same.

- Expects the sample to fail at approximately 12000.

Comments during test

- During the first cycle it was apparent that the sample started to fail/plastically deform somewhere above 60 kN. At the same point, the balance between the MEFloading also started to equal out.

- In cycle to it was clear that this was true, because the strain curves for the MEF had changed.

- After 99 cycles the loud truck horn noise occurred. Because of it I had to turn off and on the hydraulics. Some anomalies may be seen.

- At approximately 4000 cycles, the sample reaches its critical point. At the similar point the MEF strains begins to equal out.

- The sample failed at 5633 cycles.

Appendix G - Evaluation of "jumps"

Throughout the testing of several of the tests, jumps in the displacement did occur. The jumps were detected by a loud noise, accompanied by a noticeable jump in the real-time monitoring in the data acquisition software. Six jumps were detected during testing. An overview of test parameters, numbers of jumps and displaced distance is shown in table 6.

During test 5B1. The strain in the upper metal end fitting was monitored. The results have been shown together with the displacement data in figure 7. In this figure the back panel is on the same side as the one remaining bolt. Positions 1, 2 and 3 shows jump 1, 2 and 3 shown in table 6.

It is believed that the jumps occurred due to failed bolts. Because:

- The loud noise gave sounded like two metal objects being hit together.

- The side which suffered the largest strain at the end of test 5B and at the beginning of test 5C is the same side as the final bolt was on.

- The jumps only occurred on tests with higher loads.

- It is assumed that the bolts failed due to fatigue, which explains why they did not fail when subjected to higher loads during static testing.

Table 6: Displaced distance for the detected jumps.

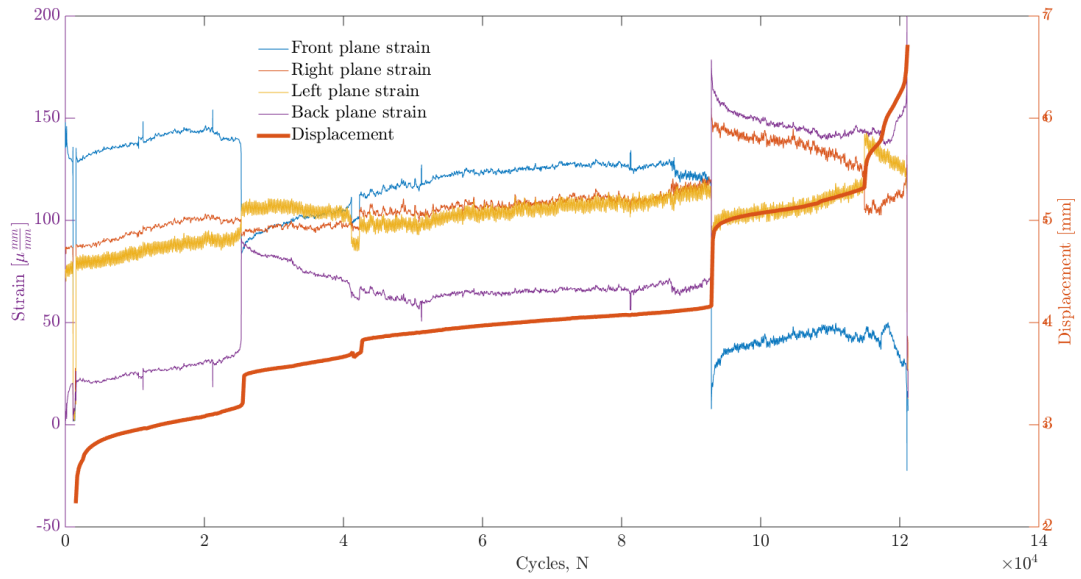| Test	Maximum load	Load frequenzy	Jump 1	Jump 2	Jump 3
4C1	90 kN	4 Hz	0.157 mm	0.429 mm	
4D1	90 kN	4 Hz	0.228 mm		
5B1	80 kN	4 Hz	0.272 mm	0.551 mm	0.158 mm

Figure 7: Strain in the upper metal end fitting compared to the overall displacement.

Appendix H - Risk Evaluation

Sikkerhets- og kvalitetsgjennomgang av laboratorietester og verkstedsarbeid
Safety and Quality Evaluation of Activities in the Laboratory and Workshop

⊙ NTNU

Perleporten

1 Identifikasjon - *Identification* | Dokumentnr. – *Document no.*:

Kundenavn – *Customer name*	Prosjektnavn – *Project name*	Projektnr. – *Project no.*
NTNU	FilaFat	62305508

Beskrivelse av arbeid – *Description of job*	Dato – *Date*
Bearbeide og utmattingsteste komposittrør, Filament winding og hand layup	08.03.2016

2 Projekt - *Team*

Prosjektleder og organisasjon – *Project manager and organisation*	Marcus Horn	Ansvarlig for instrumentering – *Responsible for instrumentation.*	Marcus Horn
Leiestedsansvarlig – *Laboratory responsible*	Marcus Horn	Operatør – *Operator*	Marcus Horn
Auditør for sikkerhets og kvalitetsgjennomgang – *Auditer for safety check*	Carl-Magnus Midtbø	Ansvarlig for styring av forsøk – *Responsible for running the experiment.*	Marcus Horn
Ansvarlig for eksperimentelt faglig innhold – *Responsible for experimental and scientific content*	Marcus Horn	Ansvarlig for logging av forsøksdata – *Responsible for logging and storing experimental data*	Marcus Horn
Ansvarlig for dimensjonering av last og trykkpåkjente komponenter – *Reponsible for dimensioning load bearing and pressurized components*	Marcus Horn	Ansvarlig for montering av testrigg – *Responsible for building the rig*	Marcus Horn

3 Viktig!! – *Important!!*

J: Ja – *Yes* / N: Nei - *No*

Er arbeidsordren signert? – *Is the work order signed?*	J
Har operatøren nødvendig kurs/trening i bruk av utstyret? - *Has the operator the required courses/training on the equipment?*	J
Har operatøren sikkerhetskurs? (påbudt) – *Has the operator followed the safety courses? (mandatory)*	J
Kan jobben gjøres alene? - *Can the work be done alone?*	J N

- Dersom ja, er det med visse forbehold (for eksempel, må bruke alarm, ha avtale med noen som kommer innom med jevne mellomrom eller lignende). Dette må vurderes i Seksjon 5.
  If yes, the work may have to be done under special conditions (e. g. must use the alarm, have agreement with somebody coming back periodically or similar). This shall be evaluated in Section 5.

4.1 Sikkerhet – *Safety* (Testen medfører – *The test contains*)

J: Ja – *Yes* / N: Nei - *No*

Stor last – *Big loads*	N	Brannfare – *Danger of fire*	N
Tunge løft – *Heavy lifting*	J	Arbeid i høyden – *Working at heights*	N
Hengende last – *Hanging load*	N	Hydraulisk trykk – *Hydraulic pressure*	J
Gasstrykk – *Gas pressure*	N	Vanntrykk – *Water pressure*	J
Høy temperatur – *High temperature*	N	Lav temperatur – *Low temperature*	N
Deler i høy hastighet – *Parts at high velocity*	J	Farlige kjemikalier – *Dangerous chemicals*	(N) ?
Sprutakselerasjon ved brudd – *Sudden acceleration at fracture/failure*	J	Forspente komponenter – *Pre-tensioned components*	J
Farlig støv – *Dangerous dust*	N	Kraftig støy – *Severe noise*	J
Klemfare – *Danger of pinching*	J	Roterende deler – *Rotating parts*	J

4.2 Påkrevet verneustyr – *Required safety equipment*

J: Ja – *Yes* / N: Nei - *No*

Briller (påbudt) – *Glasses (mandatory)*	J	Vernesko – *Safety shoes*	J
Hjelm – *Helmet*	N	Hansker – *Gloves*	N
Skjerm – *Screen*	J	Visir – *Visir*	N
Hørselsvern – *Ear protection*	J	Løfteredskap – *Lifting equipment*	N
Yrkessele, fallsele, etc. – *Harness ropes, other measures to prevent falling down.*	N		

Sikkerhets- og kvalitetsgjennomgang av laboratorietester og verkstedsarbeid

5.1 Beskrivelse av aktivitet – *Description of the activity (see Appendix)*

Vurdering skal være basert på en skriftlig prosedyre for bruk av maskinen. I enkelte tilfeller kan prosedyre bli beskrevet direkte i tabellen nedenfor.

The evaluation shall be based on a written operating procedure for the machine. For simple cases the procedure can be directly described in the tables below.

Nr.	Beskrivelse av aktiviet – *Description of activity*	Fare - *Danger*	Lov, forskrift o.l. – *Legal requirements*	Prosedyre nr. – *Procedure no.*	Sannsynlighet – *Probability*	Konsekvens – *Consequence*	Risiko – *Risk*
1	Bruk av sirkelsag	Skade på kropp	HMSregler v/ NTNU	1	3	C	3C
2	Verkstedarbeid (bade mellom 08-16 og mellom 16-08)	Sprutakselerasjon, kuttskader, klemskader, skade på maskiner	HMS-regler v/ NTNU	2	2	B	2B
3	Utmattingsteste glassfiberrør (bade mellom 08-16 og mellom 16-08)	Sprutakselerasjon ved brudd, Skade på kropp/maskiner	HMS-regler v/ NTNU	3	2	C	2C
4	Håndtering av epoxy, utføre hand layup og påføre release agent/wax (bade mellom 08-16 og mellom 16-08)	Uønsket reaksjon mellom epoxy og kropp/miljø	MSDS for gitt epoxy	4	3	C	3C
5	Sette opp filament winder for forsøk + decommission (bade mellom 08-16 og mellom 16-08)	Skade på kropp/maskiner	HMS-regler NTNU	5	2	B	2B
6	Utføre FW Jobb (bade mellom 08-16 og mellom 16-08)	Skade på kropp/maskiner Uønsket reaksjon mellom epoxy og kropp/miljø	HMS-regler NTNU	6	3	C	3C
7	Postcuring (bade mellom 08-16 og mellom 16-08)	Skade på kropp/maskiner	MSDS for gitt epoxy	7	1	B	1B

| 8 | Bruk av propangassbrenner på metall og epoxy | Skade på kropp/NTNU NTNU | HMS-regler ved NTNU | 8 | 2 | B | 1B |

5.2 Korrigerende Tiltak – Corrective Actions

Nr.	Korrigerende tiltak – Corrective action	Sannsynlighet – Probability	Konsekvens – Consequence	Risiko – Risk	Utført dato – Date of action
1	Holde avstand til sagblad, bruke hørselvern og vernebriller. Vær 2 personer.	1	A	1A	08.03.2016
2	Bruke vernebriller, forhør deg med verkstedpersonell ved nye aktiviteter, ikke bruk hansker.	1	A	1A	08.03.2016
3	Bruke skjerm og vernebriller, bruk passende grenseverdier på Instron. Sette opp klare sperrer som hindrer andre i å forstyrre prosessen.	1	A	1A	08.03.2016
4	Bruk åndedrettsvern og hansker Kast påføringsverktøy i ett lisensiert avfallsdepot. Vær 2 personer.	1	A	1A	08.03.2016
5	Vær fokusert, Unngå brå bevegelser, Vær 2 personer, vit hvor nærmeste brannslukkingsapparat er.	1	A	1A	08.03.2016
6	Ha en operatør uten hansker og en med hansker, med klare arbeidsfordelinger. Start maskin i lav hastighet.	1	A	1A	08.03.2016
7	Sette opp klare sperrer som hindrer andre i å forstyrre prosessen.	1	A	1A	08.03.2016
8	Bruke hansker og evt. tang/tvinge til håndtering, nruk gassmaske ved brenning av epoxy. Vit hvor brannslukningsapparat befinner seg.	1	A	1A	08.03.2016

5.3 Feilkilder – *Reasons for mistakes/errors*

Sjekkliste: Er følgende feilkilder vurdert? – Check list: Is the following considered?   J: Ja – *Yes* / N: Nei - *No*

Tap av strøm – *Loss of electricity*	J	Overspenning – *Voltage surge*	J
Elektromagnetisk støy – *Electromagnetic noise*	J	Manglende aggregatkapasitet av hydraulikk – *Insufficient power of the machine*	J
Jordfeil – *Electrical earth failure*	J	Vannsprut – *Water jet*	J
Ustabilt trykk av hydraulikk/kraft – *Unstable pressure or hydraulic force*	J	Tilfeldig avbrudd av hydraulikk/kraft – *Unintended interruption of power supply*	J
Last-/ forskyvnings grenser etablert ? – *Are load and displacement limits established?*	J	Lekkasjer (slanger/koblinger, etc.) – *Leakage of pipes, hoses, joints, etc.*	J
Mulige påvirkninger fra andre aktiviteter – *Possible interference from other activities*	J	Mulige påvirkninger på andre aktiviteter – *Possible interference towards other activities*	J
Problemer med datalogging og lagring – *Troubles in loading and storage*	J	Brann i laboratoriet – *Fire in the laboratory*	J

6 Kalibreringsstatus for utstyr – *Calibration of equipment*
(ex: load cell, extensometer, pressure transducer, etc)

I.D.	Utstyr - *Equipment*	Gyldig til (dato) – *Valid until (date)*
	Schenk 250 kN	?

7 Sporbarhet – *Tracebility*

Eksisterer – Is there   J: Ja – *Yes* / N: Nei - *No*

Er alle prøvematerialene kjente og identifiserbare? – *Are all experimental materials known and traceable?*	J
Eksisterer det en plan for markering av alle prøvene? – *Is there a plan for marking all specimens?*	J
Er dataloggingsutstyret identifisert? – *Is the data aquisition equipment identified?*	J
Er originaldata lagret uten modifikasjon? – *Are the original data stored safely without modification?*	J
Eksisterer det en backup-prosedyre? – *Is there a back-up procedure for the data (hard disk crash)?*	J
Eksisterer det en plan for lagring av prøvestykker etter testing? – *Is there a plan for storing samples after testing?*	J
Eksisterer en plan for avhending av gamle prøvestykker? – *Is there a plan for disposing of old samples?*	J

8 Kommentarer – *Comments*

9 Signaturer – *Signatures*
Godkjent (dato/sign) – Approved (date/signature)

Prosjektleder – *Project leader*	Verifikatør – *Verifier*	Godkjent – *Approved by*
		C-M Mdtté

Sannsynlighet vurderes etter følgende kriterier:
Probability shall be evaluated using the following criteria:

Svært liten Very unlikely 1	Liten Unlikely 2	Middels Probable 3	Stor Very Probable 4	Svært stor Nearly certain 5
1 gang/50 år eller sjeldnere – *Once per 50 years or less*	1 gang/10 år eller sjeldnere – *Once per 10 years or less*	1 gang/år eller sjeldnere – *Once a year or less*	1 gang/måned eller sjeldnere – *Once a month or less*	Skjer ukentlig – *Once a week*

Konsekvens vurderes etter følgende kriterier:
Consequence shall be evaluated using the following criteria:

Gradering – *Grading*	Menneske – *Human*	Ytre miljø, Vann, jord og luft – *Environment*	Øk/materiell – *Financial/Material*	Omdømme – *Reputation*
E **Svært Alvorlig** – *Very critical*	Død – Death	Svært langvarig og ikke reversibel skade – *Very prolonged, non-reversible damage*	Drifts- eller aktivitetsstans >1 år. – *Shutdown of work >1 year.*	Troverdighet og respekt betydelig og varig svekket – *Trustworthiness and respect are severely reduced for a long time.*
D **Alvorlig** – *Critical*	Alvorlig personskade. Mulig uførhet. – *May produce fatality/ies*	Langvarig skade. Lang restitusjonstid – *Prolonged damage. Long recovery time.*	Driftsstans > ½ år Aktivitetsstans i opp til 1 år – *Shutdown of work 0,5-1 year.*	Troverdighet og respekt betydelig svekket – *Trustworthiness and respect are severely reduced.*
C **Moderat** – *Dangerous*	Alvorlig personskade. – *Permanent injury, may produce serious health damage/sickness*	Mindre skade og lang restitusjonstid – *Minor damage. Long recovery time*	Drifts- eller aktivitetsstans < 1 mnd – *Shutdown of work < 1 month.*	Troverdighet og respekt svekket – *Troverdighet og respekt svekket.*
B **Liten** – *Relatively safe*	Skade som krever medisinsk behandling – *Injury that requires medical treatment*	Mindre skade og kort restitusjonstid – *Minor damage. Short recovery time*	Drifts- eller aktivitetsstans < 1uke – *Shutdown of work < 1 week.*	Negativ påvirkning på troverdighet og respekt – *Negative influence on trustworthiness and respect.*
A **Siker** - Safe	Injury that requires first aid	Insignificant damage. Short recovery time	Shutdown of work < 1day	

Risikoverdi = **Sannsynlighet X Konsekvenser**
Beregn risikoverdi for menneske. IPM vurderer selv om de i tillegg beregner risikoverdi for ytre miljø, økonomi/ material og omdømme. I så fall beregnes disse hver for seg.

Risk = Probability X Consequence
Calculate risk level for humans. IPM shall evaluate itself if it shall calculate in addition risk for the environment, economic/material and reputation. If so, the risks shall be calculated separately.

Risikomatrisen
Risk Matrix

I risikomatrisen er ulike grader av risiko merket med rød, gul eller grønn:

Rød: Uakseptabel risiko. Tiltak skal gjennomføres for å redusere riskoen.

Gul: Vurderingsområde. Tiltak skal vurderes.

Grønn: Akseptabel risiko. Tiltak kan vurderes ut fra andre hensyn.

Når risikoverdien havner på rødt felt, skal altså enheten gjennomføre tiltak for å redusere risikoen. Etter at tiltak er iverksatt, skal dere foreta ny risikovurdering for å se om risikoen har sunket til akseptabelt nivå.

For å få oversikt over samlet risiko: Skriv risikoverdi og aktivitetens IDnr. i risikomatrise (docx) / risikomatrise (odt). Eksempel: Aktivitet med IDnr. 1 har fått risikoverdi 3D. I felt 3D i risikomatrisen skriver du IDnr. 1. Gjør likedan for alle aktiviteter som har fått en risikoverdi. En annen måte å skaffe oversikt på, er å fargelegge feltet med risikoverdien i skjemaet for risikovurdering. Dette tydeliggjør og gir samlet oversikt over riskoforholdene. Ledelse og brukere får slik et godt bilde av risikoforhold og hva som må prioriteres.

In the risk matrix different degrees of risk are marked with red, yellow or green;

Red: Unacceptable risk. Measures shall be taken to reduce the risk.

Yellow: Assessment Area . Measures to be considered.

Green: Acceptable risk. Measures can be evaluated based on other considerations.

When a risk value is red, the unit shall implement measures to reduce risk. After the action is taken, you will make a new risk assessment to see if the risk has decreased to acceptable levels.

To get an overview of the overall risk: Write the risk value and the task ID no . the risk matrix (docx) / risk matrix (odt) . Example : Activity with ID no . 1 has been risk value 3D. In the field of 3D risk matrix type ID no . 1 Do the same for all activities that have been a risk . Another way to get an overview is to color the field of risk value in the form of risk assessment . This clarifies and gives overview of the risk factors . Management and users get such a good picture of the risks and what needs to be prioritized.

KONSEKVENS	Svært alvorlig	E1	E2	E3	E4	E5
	Alvorlig	D1	D2	D3	D4	D5
	Moderat	C1	C2	C3	C4	C5
	Liten	B1	B2	B3	B4	B5
	Svært liten	A1	A2	A3	A4	A5
		Svært liten	Liten	Middels	Stor	Svært stor
		SANNSYNLIGHET				

Prinsipp over akseptkriterium. Forklaring av fargene som er brukt i risikomatrisen.

Farge		Beskrivelse
Rød		Uakseptabel risiko. Tiltak skal gjennomføres for å redusere risikoen.
Gul		Vurderingsområde. Tiltak skal vurderes.
Grønn		Akseptabel risiko. Tiltak kan vurderes ut fra andre hensyn.

Til Kolonnen "Korrigerende Tiltak":

Tiltak kan påvirke både sannsynlighet og konsekvens. Prioriter tiltak som kan forhindre at hendelsen inntreffer, dvs sannsynlighetsreduserende tiltak foran skjerpende beredskap, dvs konsekvensreduserende tiltak.

For Column "Corrective Actions"
Corrections can influence both probability and consequence. Prioritize actions that can prevent an event from happening.

Oppfølging:

Tiltak fra risikovurderingen skal følges opp gjennom en handlingsplan med ansvarlige personer og tidsfrister.

Follow Up
Actions from the risk evaluation shall be followed through by an action plan with responsible persons and time limits.

Etterarbeid #

- Gå gjennom aktiviteten/prosessen på nytt.
- Foreta eventuell ny befaring av aktiviteten/prosessen for enten a) å få bekreftet at risikoverdiene er akseptable eller b) for å justere risikoverdiene.
- Gå gjennom, vurder og prioriter tiltak for å forebygge uønskede hendelser. Først skal dere prioritere tiltak som reduserer sannsynlighet for risiko. Dernest skal dere ta for dere tiltak som reduserer risiko for konsekvenser.
- Tiltakene skal føres inn i handlingsplanen. Skriv fristen for å gjennomføre tiltaket (dato, ikke tidsrom) og navn på den / de som har ansvar for tiltakene.
- Foreta helhetsvurdering for å avgjøre om det nå er akseptabel risiko.
- Ferdig risikovurdering danner grunnlag for å utarbeide lokale retningslinjer og HMS-dokumenter, opplæring og valg av sikkerhetsutstyr.
- Ferdig risikovurdering og eventuelle nye retningslinjer gjøres kjent/tilgjengelig for alle involverte.
- Sett eventuelt opp kostnadsoverslag over planlagte tiltak.